

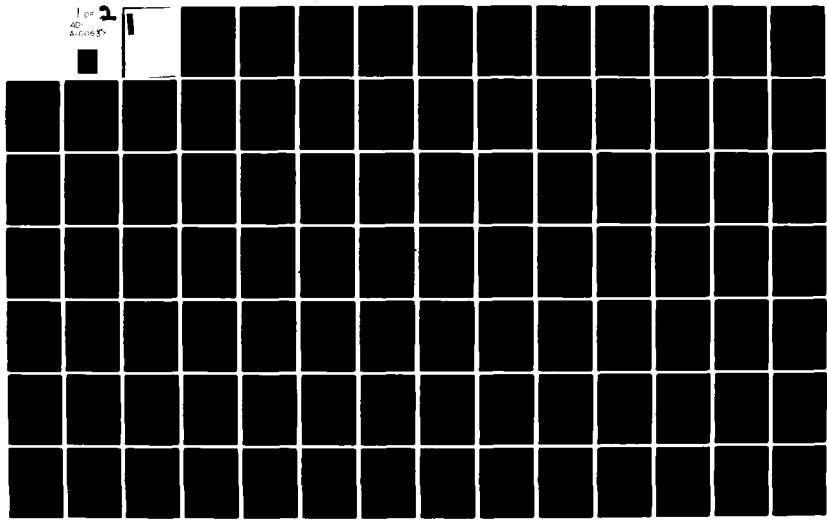
AD-A100 637

AIR FORCE INST OF TECH WRIGHT-PATTERSON AFB OH SCHO00--ETC F/G 12/1  
RADHOT: A RADIATION HYDRODYNAMICS CODE FOR WEAPON EFFECTS CALCULUS--ETC(U)  
MAR 81 D P WADE

UNCLASSIFIED AFIT/GNE/PH/81-10

NL

1 of 3  
AD-A100 637



AD A100637

II

①

RADHOT: A RADIATION  
HYDRODYNAMICS CODE FOR  
WEAPON EFFECTS CALCULATION

THESIS

AFIT/GNE/PH/81-10

Douglas P. Wade  
Captain USAF

RADHOT: A RADIATION  
HYDRODYNAMICS CODE FOR  
WEAPON EFFECTS CALCULATION

THESIS

Presented to the Faculty of the School of Engineering  
of the Air Force Institute of Technology  
in Partial Fulfillment of the  
Requirements for the Degree of  
Master of Science

by  
Douglas P. Wade  
Captain USAF  
Graduate Nuclear Engineering  
March 1981

A

Preface

This report contains the results of my efforts to develop a computer code capable of describing the time dependent blast overpressure and temperature profile resulting from the detonation of a nuclear weapon in the lower atmosphere. The code is not fully working at this time, due in part to the lack of valid opacity data at the temperatures of interest. The code is highly modular, and can serve as a starting point should this work be continued in the future.

I would like to thank my advisor, Captain David Hardin, for his guidance and his patient, frequently repeated, explanations throughout the research period. Most of all, I would like to thank my wife, Carol, for her patience, love and understanding throughout the period of this work.

Douglas P. Wade

## Contents

Preface.....	ii
List of Figures.....	iv
List of Notation.....	v
Abstract.....	vii
I.    Introduction.....	1
II.   Radiation Hydrodynamic Finite Difference Scheme.....	4
Theory.....	4
Development of Radiation Difference Scheme.....	14
Hydrodynamic Finite Difference Scheme....	38
III.  Timestep, Equation of State, and Opacity....	43
Timestep Criteria.....	43
Equations of State.....	45
Temperature Approximation.....	45
Opacity.....	49
IV.   Problem Definition and Solution.....	55
V.    Results and Discussion.....	62
VI.   Conclusions and Recommendations.....	72
Conclusions.....	72
Recommendations.....	73
Bibliography.....	74
Appendix A: Derivations.....	75
Appendix B: Users Guide for RADHOT.....	77
Appendix C: Program Listing of RADHOT.....	80
Vita.....	94

List of Figures

1.	Equation of Radiative Transfer, Geometry.....	8
2.	Integral Radiative Transport Equation, Geometry.....	9
3.	Finite Difference Labeling Scheme.....	15
4.	Finite Difference Equation of Radiative Transfer, Geometry.....	16
5.	Angular Relations.....	18
6.	Distance Across a Cell.....	22
7.	Monochromatic Intensity Distribution.....	27
8.	Radiation Transport Labeling Scheme.....	29
9.	Plot of Z* vs Temperature.....	48
10.	Plot of Absorbtion Coefficient vs Photon Energy.....	50
11.	Absorbtion Coefficient in Air, Ambient Density.....	51
12.	Absorbtion Coefficient in Air, 1/1000 Ambient Density.....	52
13.	Program RADHOT Flow Diagram.....	59
14.	1MT BLAST, $10^{-7}$ .....	64
15.	1MT BLAST, $7.6 \times 10^{-4}$ sec.....	65
16.	1MT BLAST, $2.7 \times 10^{-3}$ sec.....	67
17.	1MT BLAST, $4.5 \times 10^{-3}$ sec.....	68
18.	1MT BLAST, $\mu'$ FIXED, $10^{-7}$ sec.....	70
19.	1MT BLAST, $\mu'$ FIXED, $7.6 \times 10^{-4}$ sec.....	71

### List of Notation

a	number of cells the shock front is spread over
$a_{i+\frac{1}{2}}$	acceleration of cell boundary
$B_v$	Planck function
$E_m$	internal energy
$\frac{\partial E_m}{\partial t} \Big _{rad}$	rate of change of internal energy due to radiation
$F_v$	monochromatic flux
$F_v^-$ , $F_v^+$	inward and outward-going monochromatic fluxes at a cell boundary
$F_1^-$ , $F_1^+$	inward and outward-going fluxes at the inner cell boundary
$F_2^-$ , $F_2^+$	inward and outward-going fluxes at the outer cell boundary
h	Planck constant
I	internal energy
$I_v$	monochromatic radiation intensity
$I_1$ , $I_2$	intensity of a ray at the inner and outer cell boundaries
k	Boltzmann constant
$m_i$	mass in a cell
p	pressure
$P_1$ , $P_2$	points along a specified ray
Q	artificial viscous pressure
r	radius from center of symmetry
$R_0$	initial mesh spacing
$R_1$ , $R_2$	inner and outer cell boundaries
$\Delta R$	cell thickness
$\Delta s$	differential length
$\Delta s(\theta)$	distance across a cell in a specified direction
T	temperature
$\Delta t$	radiation timestep
$\Delta t_H$	hydrodynamic timestep

$U_i$	cell boundary velocity
$U(\theta)$	$\mu' \Delta s(\theta)$
$V$	volume or specific volume
$\vec{v}$	velocity
$\gamma$	equation of state variable
$\theta$	angle between radius vector and a ray passing thru the mesh
$\theta_1, \theta_2$	angle between radius vector and a specified ray at the inner and outer cell boundaries
$\theta_m$	maximum value of $\theta_2$ for a ray that will intersect the inner boundary
$\mu'$	radiative absorbtion coefficient corrected for stimulated emmission
$\nu$	frequency
$d\xi, d\xi'$	differential distance along a specified ray
$\rho$	density
$\rho_0$	initial cell density
$\omega$	element of solid angle

Abstract

RADHOT is a one-dimensional Lagrangian radiation-hydrodynamics computer code developed from a scheme described by John Zinn of LASL. The transport scheme described by John Zinn and incorporated into RADHOT requires just two passes thru the mesh to determine fluxes and energy deposition rates. The scheme assumes local thermodynamic equilibrium for each cell, and also assumes that the thermal radiation flux contribution in a given direction at any point has one of two values depending upon whether a ray in that direction intersects the source region.

The RADHOT code is believed to be "debugged," but suffers from a lack of valid opacity and equation of state information. Because of this, no comparisons can be made. Also, the code as currently written is extremely slow and expensive to run. A users guide and a listing of the code are provided as a starting point for future work.

RADHOT: A RADIATION  
HYDRODYNAMICS CODE FOR  
WEAPON EFFECTS CALCULATION

I Introduction

Nuclear explosives are characterized by the very rapid release of large quantities of energy into a small volume. Initially, the released energy is primarily in the form of thermal radiation. As the thermal radiation streams away from the source, it is continuously absorbed and re-emitted by the surrounding atmosphere. With each absorption/re-emission, a fraction of the thermal energy will be transformed into material energy. The increase in material energy is manifested as a pressure gradient between the "absorption" region and the surrounding, undisturbed region. This pressure differential results in a shock wave being initiated (Ref 1). Large overpressures associated with the shock wave, together with thermal radiation fluxes are major damage mechanisms of a nuclear explosion. An understanding of the physics involved is essential to producing a model to predict weapon effects.

The difference equations of "shock" hydrodynamics are developed by Richtmeyer (Ref 2) and are well understood. However, at early times after detonation when radiation energy is significant,

and certainly prior to  $\sim 10^{-4}$  sec. (radiative expansion phase), the hydrodynamic equations must be modified to include radiation transport (Ref 3).

The primary purpose of this thesis was to develop a computer code capable of predicting the weapon effects (overpressures, temperatures and radiation fluxes) resulting from a 1KT - 1MT nuclear explosion. The computer code was to account for radiation transport at early times, between  $\sim 10^{-7}$  sec. to 10 sec. after detonation.

An existing hydrodynamics code, HUFF, was used as a starting point for this thesis, and RADHOT incorporates some of HUFF's subroutines (Ref 4). HUFF utilized a 1-D Lagrangian mesh to solve shock hydrodynamic problems in the absence of radiation heating. At times later than  $10^{-2}$  sec. after detonation, HUFF is accurate to within ~5%. At earlier times, HUFF's accuracy decreases, and because HUFF lacks any provisions for radiation transport, it is incapable of making any predictions prior to  $\sim 10^{-4}$  sec. RADHOT incorporates the I/O routines and the Lagrangian hydro scheme from HUFF, as well as a fit to the Nickel-Doan Equation of State (EOS) for Air (Ref 5).

The radiation transport scheme in RADHOT was developed by John Zinn of LASL (Ref 6). In Zinn's scheme radiation fluxes at the cell boundaries are determined at each time step by making two passes through the mesh. The radiation fluxes are then used to determine source terms which are input into the hydro scheme.

Detailed development of Zinn's transport scheme together with the assumptions and approximations behind it are presented in chapter II as is the associated hydro scheme. This development comprises a major portion of this thesis. Chapter III discusses the timestep constraints in RADFLO together with the equation of state and opacity approximations. The organization of RADFLO is discussed in chapter IV, and chapter V discusses the results obtained and reasons for the lack of correlation to data. Finally, chapter VI contains the conclusions and recommendations of this study.

## II Radiation Hydrodynamic Finite Difference Scheme

### Theory

"Thermal radiation" is electromagnetic radiation emitted by matter in a state of thermal excitation. The energy density of such radiation is defined by the Planck formula:

$$B(\nu, T) = \frac{2h\nu^3}{c^2} \left( e^{\frac{h\nu}{kT}} - 1 \right)^{-1} \quad (1)$$

where  $\nu$  is frequency,  $T$  is temperature,  $B$  is the Planck function ( $\text{ergs/cm}^2$ ),  $c$  is the speed of light and  $h$  and  $k$  are the Planck and Boltzmann constants respectively. The importance of thermal radiation increases as the temperature is raised. At moderate temperatures, its role is primarily one of transmitting energy, whereas at high temperatures the energy density of the radiation field itself becomes important as well. If thermal radiation must be considered explicitly in a problem, the radiative properties of matter must be known. A determination of the radiative properties usually requires an assumption that "local thermodynamic equilibrium" (LTE) exists. Whenever thermal radiation is considered, the medium that contains it inevitably has pressure and density gradients and the treatment requires the use of hydrodynamics. Hydrodynamics with explicit consideration of thermal radiation is called "radiation hydrodynamics," (Ref 7).

John Zinn of LASL has developed a computational method for the time-dependent radiation hydrodynamic environment

encountered after the detonation of a nuclear weapon in the lower atmosphere. The growth of a nuclear fireball can be computed within certain limitations using the finite difference scheme that he describes. Zinn's scheme is restricted to problems with spherical symmetry. The scheme requires just two passes through the mesh to determine incoming and out-going fluxes, and therefore, the scheme should be relatively fast on a computer.

Zinn makes a number of simplifying assumptions in the scheme, the first of which is the standard one requiring that LTE exists in each mesh cell so that local absorption coefficients can be expressed as functions of local temperature and density. Zinn disregards radiation energy density and radiation pressure terms in the equation of state, accepting errors at times less than  $10^{-7}$  sec. because of the omission. Zinn ignores photon time-of-flight effects, justifying the omission because the transit time of photons across a cell is small compared to the e-folding time for the exchange of energy between the matter and radiation field. Finally, Zinn starts his scheme by placing all of the energy of the weapon in the first cell at  $t = 10^{-7}$  sec. after detonation and restricting the thermal radiation from crossing the cell boundary until after that time. This prevents any preheating of the next cell. Again, the principal effect of this is to introduce a timing error into the system.

Zinn's radiation transport scheme assumes that the angular distribution of the monochromatic radiation intensities (and

therefore the fluxes) are either 1) approximately isotropic, such as in an "optically thick" region or in an "optically thin" region bounded by two "optically thick" regions, or 2) can be approximated by a function that has one of two values, such as encountered in the cool transparent region outside of an "optically thick" source. The transport scheme determines the inward-going and outward-going fluxes at each cell boundary for a large number of frequency groups. By using a large number of frequency groups, a more accurate determination of the radiative absorption coefficient  $\mu'$  can be made. An accurate determination of  $\mu'$  is essential to defining "optically thick," and therefore to defining the source region. An accurate determination of the source region is important to the overall accuracy of the scheme.

The equation of radiative transfer, also called the transport equation, is a mathematical statement of conservation. The equation of radiative transfer says

$$\frac{\text{change in intensity}}{\text{per unit distance}} = \frac{\text{transfer of energy to radiant energy}}{\text{material energy}} - \frac{\text{attenuation of radiation energy}}{\text{(conversion to material energy)}}. \quad (2)$$

with the restrictions already noted, the equation of radiative transfer can be stated

$$\frac{\partial I_v}{\partial s} = \cos\theta \frac{\partial I_v}{\partial r} - \frac{\sin\theta}{r} \frac{\partial I_v}{\partial \theta} = \mu' (B_v - I_v) \quad (3)$$

where

$I_v$  = radiation intensity at frequency  $v$

$\theta$  = angle between the radius vector and  
the direction of the ray contributing  
to the intensity

$ds$  = differential distance along the ray  
in the direction of travel

$r$  = distance from center of symmetry

$\mu'$  = absorbtion coefficient corrected  
for stimulated emmission

$B_v$  = Planck function

See Fig 1.

Now, Pomraning (Ref 8:27) shows that the differential equation of radiative transfer (equation 3) can be replaced by an equivalent integral equation. The integral equation or radiative transfer is,

$$I_v(P_2) = I_v(P_1) e^{-\int_{P_1}^{P_2} \mu'(\xi) d\xi}$$
$$+ \int_{P_1}^{P_2} \mu'(\xi) B_v(\xi) e^{-\int_{\xi}^{P_2} \mu'(\xi') d\xi'} d\xi \quad (4)$$

where  $d\xi$  and  $d\xi'$  are elements of distance along the ray connecting  $P_1$  and  $P_2$ . See Fig 2. In words, equation (4) says that at any point  $P_2$ , the intensity contribution at that point from any other point  $P_1$  is equal to the initial intensity at  $P_1$  in the direction of  $P_2$ , less any attenuation of the initial intensity between  $P_1$  and  $P_2$ , plus any re-emmission

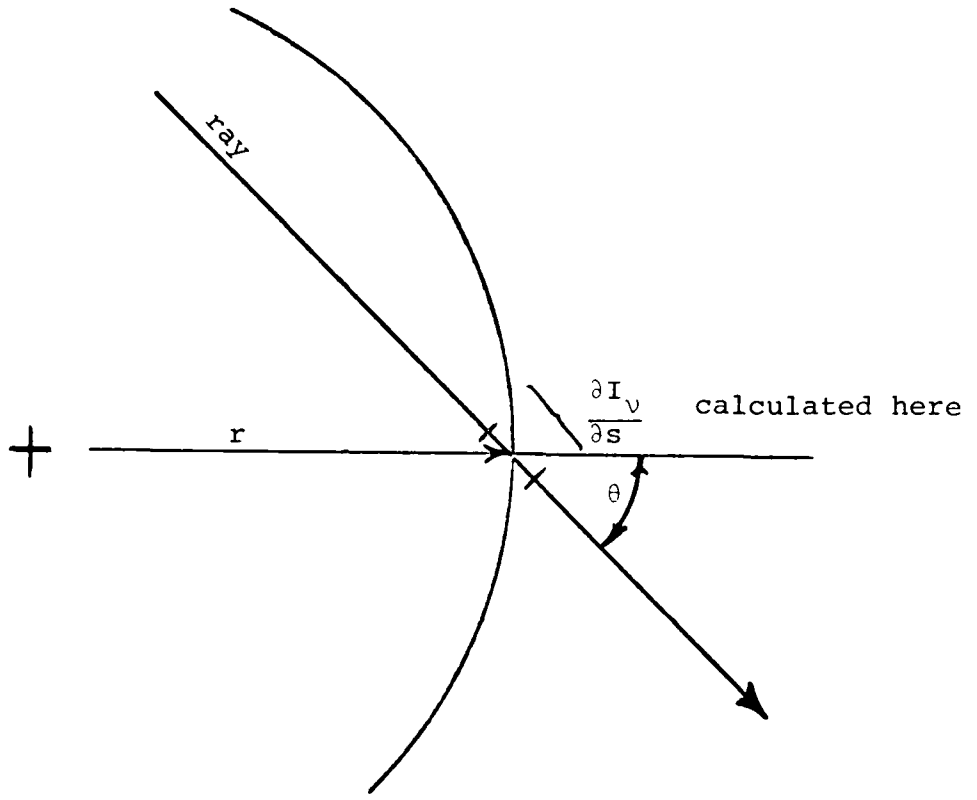


Fig 1. Equation of Radiative Transfer, Geometry

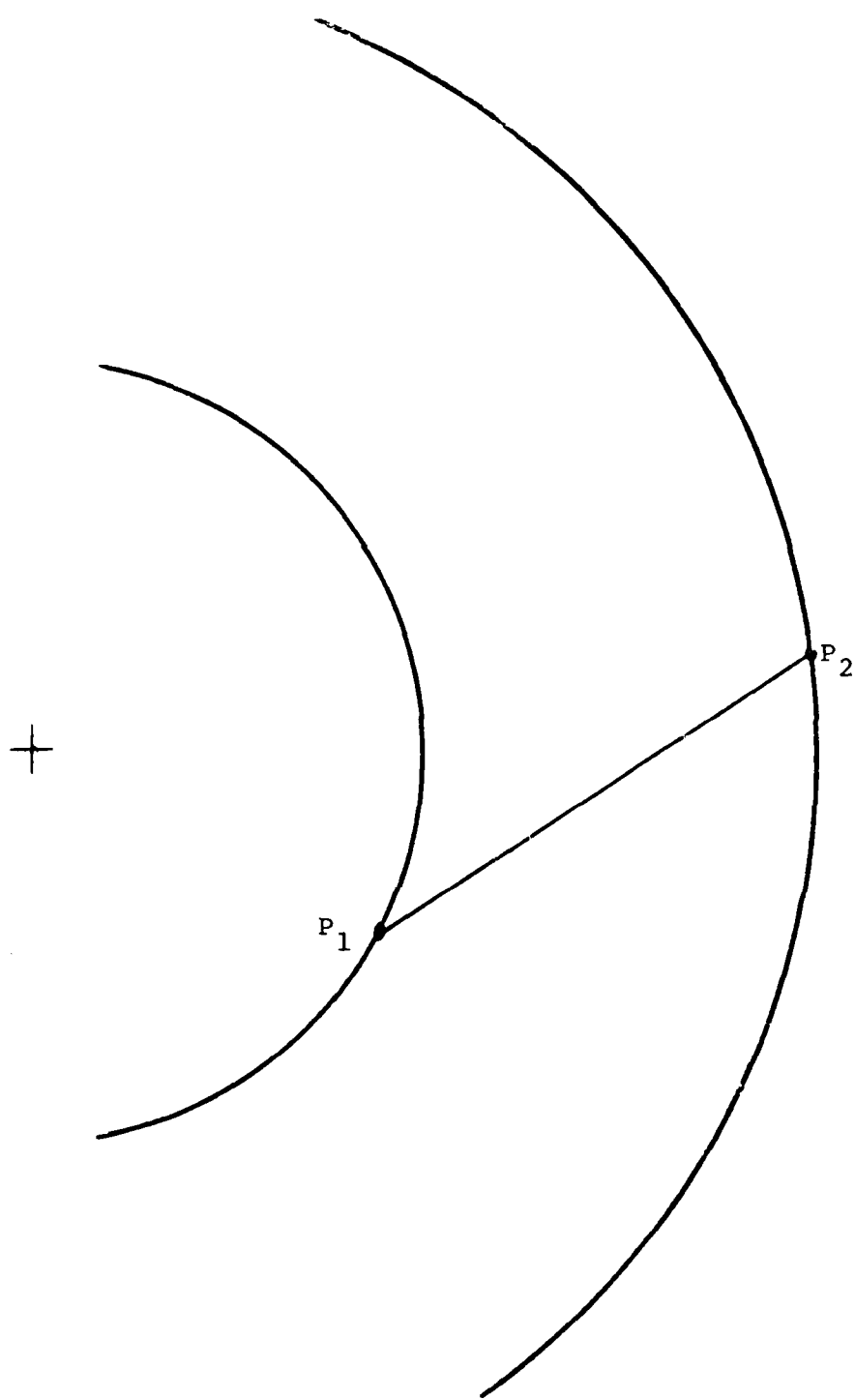


Fig 2. Integral Equation of Radiative Transfer, Geometry

of radiation in the direction of  $P_2$  along the path from  $P_1$  to  $P_2$ , less any attenuation of the re-emitted radiation.

The rate at which the material energy of the system is increased by the absorption and re-emission of radiation is,

$$\frac{\partial E_m}{\partial t} \Big)_{rad} = \int_0^\infty \mu' \left( \int_{4\pi} I_v d\omega - 4\pi B_v \right) dv \quad (5)$$

where

$\mu' \int_{4\pi} I d\omega$  represents radiation energy lost to material energy

and

$4\pi\mu' B_v$  represents material energy being given up to the radiation field.

For the transport scheme being developed, the flux,  $F_v$ , is calculated instead of the intensity  $I_v$ . Since the transport scheme is restricted to problems with spherical symmetry, the two quantities are related by,

$$F_v = 2\pi \int_0^\pi I_v(\theta) \sin\theta \cos\theta d\theta \quad (6)$$

For problems with spherical symmetry, equation (5) can be expressed more simply, since

$$d\omega = 2\pi \sin\theta d\theta. \quad (7)$$

Let

$$\cos\theta = \omega, \quad \text{therefore,}$$

$$F_v = \int_{4\pi} \omega I_v d\omega \quad (8)$$

Now,

$$\omega \cdot \nabla I_v - \mu' I_v + \mu' B_v = 0 \quad (9)$$

where  $\omega \cdot \nabla I_v$  is the net leakage out of a volume,  $-\mu' I$  represents the loss of radiation due to absorption, and  $\mu' B_v$  is a source term. Then,

$$-\omega \cdot \nabla I_v = \mu' (B_v - I_v) = \frac{\partial I_v}{\partial s}. \quad (10)$$

Integrating equation (10) with respect to solid angle yields

$$-\nabla \cdot \int_{4\pi} \omega I_v d\omega = \mu' \left[ B_v \int_{4\pi} d\omega - \int_{4\pi} I_v d\omega \right] \quad (11)$$

or,

$$-\nabla \cdot \vec{F} = \mu' \left[ 4\pi B_v - \int_{4\pi} I_v d\omega \right]. \quad (12)$$

Therefore, equation (5) can be written as

$$\frac{\partial E_m}{\partial t} \Big|_{rad} = - \int_0^\infty \nabla \cdot \vec{F}_v \, dv \quad (13)$$

With the inclusion of equation (13), the equations of radiation hydrodynamics are, the conservation of mass equation,

$$\frac{\partial \rho}{\partial t} = -\nabla \cdot (\rho \vec{v}); \quad (14)$$

the conservation of momentum equation,

$$\frac{\partial (\rho \vec{v})}{\partial t} = -\nabla \cdot (\rho \vec{v} \vec{v}) - \nabla P; \quad (15)$$

and the conservation of energy equation,

$$\frac{\partial E_m}{\partial t} = -\nabla \cdot (E_m \vec{v}) - P \nabla \cdot \vec{v} - \int_0^\infty \nabla \cdot \vec{F}_v \, dv. \quad (16)$$

These equations, coupled with the transport equation, equation (4) are the set for which a finite difference scheme will be developed to solve.

Equations 13-16 are a closed set, upon specification of the equation of state relations:

$$P = \text{pressure} = P(\rho, E_m), \quad (17)$$

$$T = \text{temperature} = T(\rho, E_m), \quad (18)$$

the radiative absorption coefficients

$$\mu' = \mu'(\rho, E_m, v) \quad (19)$$

and the definition of the flux and Planck functions (equations 6 and 1).

## Radiation Transport Finite Difference Formulation

The finite difference mesh for the category of problems addressed in this thesis consists of a series of 100 concentric shells. Initially the thickness of each shell is constant, though because a Lagrangian hydro scheme is being implemented, cell boundaries will be continually readjusted during the course of the problem to conserve mass. Initially, all except the first cell will contain air at ambient temperature and pressure. The first cell initially contains the mass of the weapon (1000 kg) at a temperature and pressure consistent with the weapon yield. See Fig 3 for the mesh labeling scheme. Beginning at  $10^{-7}$  sec. after detonation, radiation energy is allowed to propagate through the mesh. The equations governing the radiation transport will be developed below.

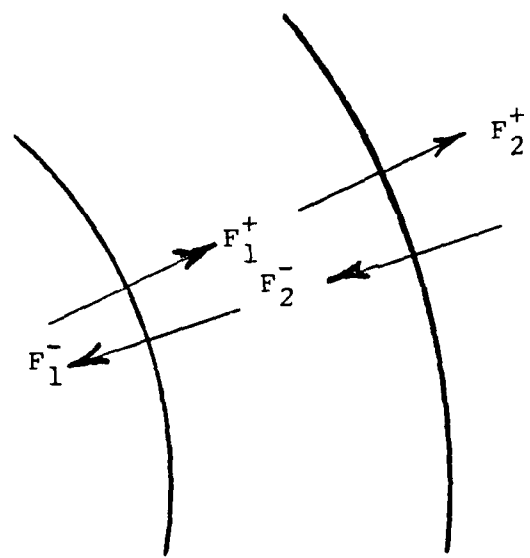
At a specific instant in time, the contribution to the intensity  $I_v$  at a point  $P_2$  on the surface of a volume element from any other arbitrary point  $P_1$  on the same surface in a given direction is:

$$I_v(P_2) = I_v(P_1)e^{-\mu' \Delta s} + B_v(1-e^{-\mu' \Delta s}) \quad (20)$$

as illustrated in Fig 4.

This is an approximation to the more exact equation (4)

developed in the last section. Specifically,  $\int_{P_1}^{P_2} \mu'(\xi) d\xi$



$X(I)$	$X(I+1)$
$VEL(I)$	$VEL(I+1)$
$P(I)$	$P(I+1)$
$\tau(I)$	$\tau(I+1)$
$\rho(I)$	$\rho(I+1)$
$B_v(I)$	$B_v(I+1)$
$u'(I)$	$u'(I+1)$
$E_m(I)$	$E_m(I+1)$

Fig 3. Finite Difference Labeling Scheme

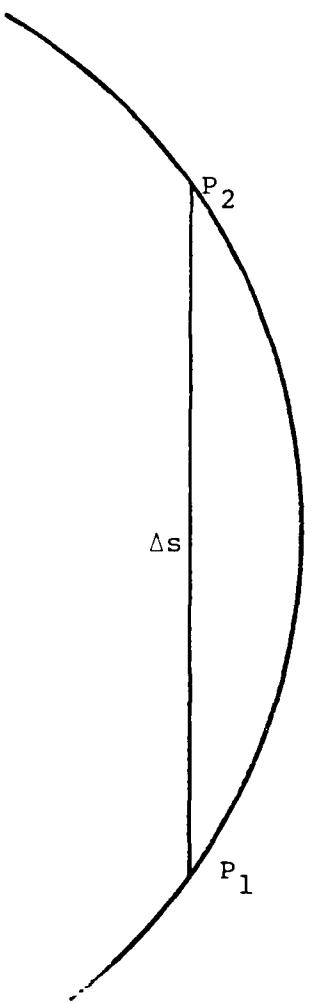


Fig 4. Finite Difference Equation of Radiative Transfer,  
Geometry

is approximated by  $\mu' \Delta s$  and  $\int_{P_1}^{P_2} B_v \mu'(\xi) e^{-\int_{\xi}^{P_2} \mu'(\xi') d\xi'} d\xi'$

is approximated by  $B_v(1 - e^{\mu' \Delta s})$ . The dependence of  $\mu'$  and  $B_v$  on the differential element of length  $\xi$  disappears because of the assumption of local thermodynamic equilibrium.

$\theta_1$  and  $\theta_2$  are shown in Fig 5, where a ray is depicted crossing the cell.  $\theta_1$  and  $\theta_2$  are related via

$$R_1 \sin \theta_1 = R_2 \sin \theta_2 \quad (21)$$

Letting  $I_1(\theta_1)$  and  $I_2(\theta_2)$  be the intensities of a given ray at locations  $R_1$  and  $R_2$  and  $\Delta s(\theta_2)$  be the distance between  $R_1$  and  $R_2$  along the ray, then an angle  $\theta_m$  can be defined for  $\theta_2$  such that

$$\theta_m = \sin^{-1} (R_1/R_2) \quad (22)$$

which is the maximum value of  $\theta_2$  for rays that still intersect  $R_1$  (i.e. the  $R_1$  surface is grazed and  $\theta_1 = 90^\circ$ ).

The above equations can now be used to define the outward flux at  $R_2$ .

The out-going and in-going fluxes at each shell surface (cell boundary) are:

$$F_v^+ = 2\pi \int_0^{\pi/2} I_v(\theta) \sin \theta \cos \theta d\theta \quad (23)$$

$$F_v^- = -2\pi \int_{\pi/2}^{\pi} I_v(\theta) \sin \theta \cos \theta d\theta \quad (24)$$

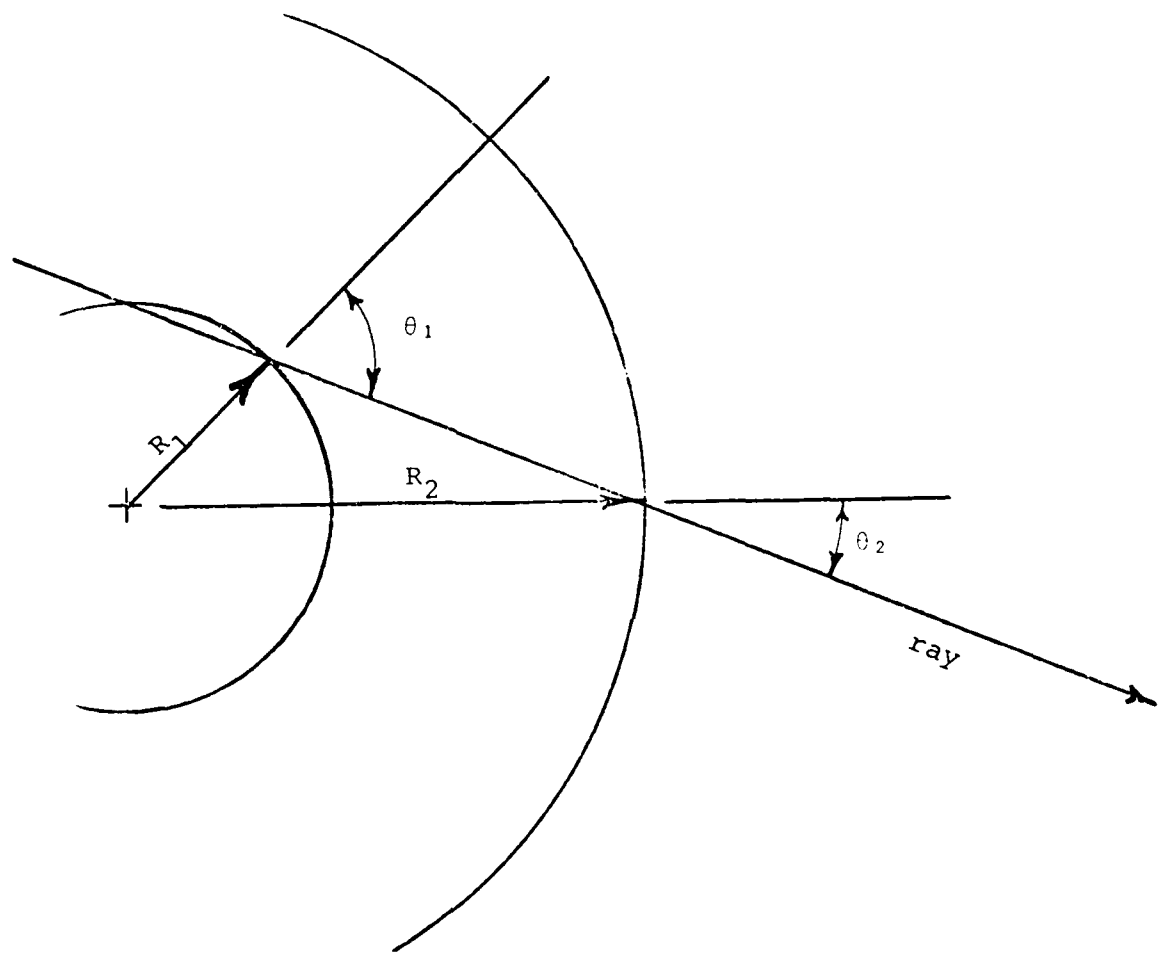


Fig 5. Angular Relationships

Using equations (18), (21), (22), the outward flux at  $R_2$  is:

$$I_v(P_2) = I_2(P_1)e^{-\mu' \Delta s} + B_v(1-e^{-\mu' \Delta s}) \quad (20)$$

$$F_v^+ = 2\pi \int_0^{\pi/2} I_v(\theta) \sin\theta \cos\theta d\theta \quad (23)$$

Therefore,

$$\begin{aligned} F_{2,v}^+ &= 2\pi \int_0^{\theta_m} I_1(\theta_1) e^{-\mu' \Delta s(\theta_2)} \sin\theta_2 \cos\theta_2 d\theta_2 \\ &+ 2\pi \int_0^{\theta_m} B_v(1-e^{-\mu' \Delta s(\theta_2)}) \sin\theta_2 \cos\theta_2 d\theta_2 \\ &+ 2\pi \int_{\theta_m}^{\pi/2} I_1(\pi-\theta_2) e^{-\mu' \Delta s(\theta_2)} \sin\theta_2 \cos\theta_2 d\theta_2 \\ &+ 2\pi \int_{\theta_m}^{\pi/2} B_v(1-e^{-\mu' \Delta s(\theta_2)}) \sin\theta_2 \cos\theta_2 d\theta_2 \end{aligned} \quad (25)$$

Reducing,

$$\begin{aligned} F_{2,v}^+ &= 2\pi \int_0^{\theta_m} I_1(\theta_1) e^{-\mu' \Delta s(\theta_2)} \sin\theta_2 \cos\theta_2 d\theta_2 \\ &+ B_v \left[ \pi \sin^2 \theta_m - 2\pi \int_0^{\theta_m} e^{-\mu' \Delta s(\theta_2)} \sin\theta_2 \cos\theta_2 d\theta_2 \right] \end{aligned}$$

$$\begin{aligned}
& + 2\pi \int_{\theta_m}^{\pi/2} I_2(\pi - \theta_2) e^{-\mu' \Delta s(\theta_2)} \sin \theta_2 \cos \theta_2 d\theta_2 \\
& + B_v \left\{ \cos^2 \theta_m - 2\pi \int_{\theta_m}^{\pi/2} e^{-\mu' \Delta s(\theta_2)} \sin \theta_2 \cos \theta_2 d\theta_2 \right\} \quad (26)
\end{aligned}$$

For the inward-going flux at  $R_1$ , only those rays with incident angles less than  $\theta_m$  will make a contribution.

Starting with

$$F_1^- = -2\pi \int_{\pi/2}^{\pi} I_1(\theta_1) \cos \theta_1 \sin \theta_1 d\theta_1, \quad (24)$$

and from equation 21,

$$\sin \theta_1 = R_2/R_1 \sin \theta_2 \quad (27)$$

$$I(\theta_1) = I(\theta_2) e^{-\mu' \Delta s} + B(1 - e^{-\mu' \Delta s}) \quad (28)$$

$$\cos \theta_1 d\theta_1 = R_2/R_1 \cos \theta_2 d\theta_2 \quad (29)$$

$$\sin \theta_1 \cos \theta_1 d\theta_1 = (R_2/R_1)^2 \cos \theta_2 \sin \theta_2 d\theta_2 \quad (30)$$

and from equation 22,

$$(R_2/R_1)^2 = 1/\sin^2 \theta_m \quad (31)$$

therefore,

$$\sin\theta_1 \cos\theta_1 d\theta_1 = \sin\theta_2 \cos\theta_2 / \sin^2\theta_m d\theta_2 \quad (32)$$

changing the limits of integration,

$$\text{if } \theta_1 = \pi, \text{ then } \theta_2 = \pi \quad (33)$$

$$\text{if } \theta_1 = \pi/2, \text{ then } \theta_2 = \pi - \theta_m \quad (34)$$

combining (24) with (28), and remembering that the only rays that make a contribution to the flux at  $R_1$  are those whose incident angles are less than or equal to  $\theta_m$ , then,

$$\begin{aligned} F_1^- &= -2\pi \int_{\theta_m}^{\pi} I_2(\pi-\theta_2) e^{-\mu' \Delta s(\theta_2)} \sin\theta_2 \cos\theta_2 / \sin^2\theta_m d\theta_2 \\ &- 2\pi B \int_{\theta_m}^{\pi} \{1-e^{-\mu' \Delta s(\theta_2)}\} \sin\theta_2 \cos\theta_2 / \sin^2\theta_m d\theta_2 \end{aligned} \quad (35)$$

or,

$$\begin{aligned} F_1^- &= 2/\sin^2\theta_m \int_0^{\theta_m} I_2(\pi-\theta_2) e^{-\mu' \Delta s(\theta_2)} \sin\theta_2 \cos\theta_2 d\theta_2 \\ &+ \pi B \left\{ 1-2/\sin^2\theta_m \int_0^{\theta_m} e^{-\mu' \Delta s(\theta_2)} \sin\theta_2 \cos\theta_2 d\theta_2 \right\} \end{aligned} \quad (36)$$

Now, it is necessary to determine  $\Delta s(\theta_2)$ . For angles such that  $0 \leq \theta_2 < \theta_m$  as shown in Fig 6a.

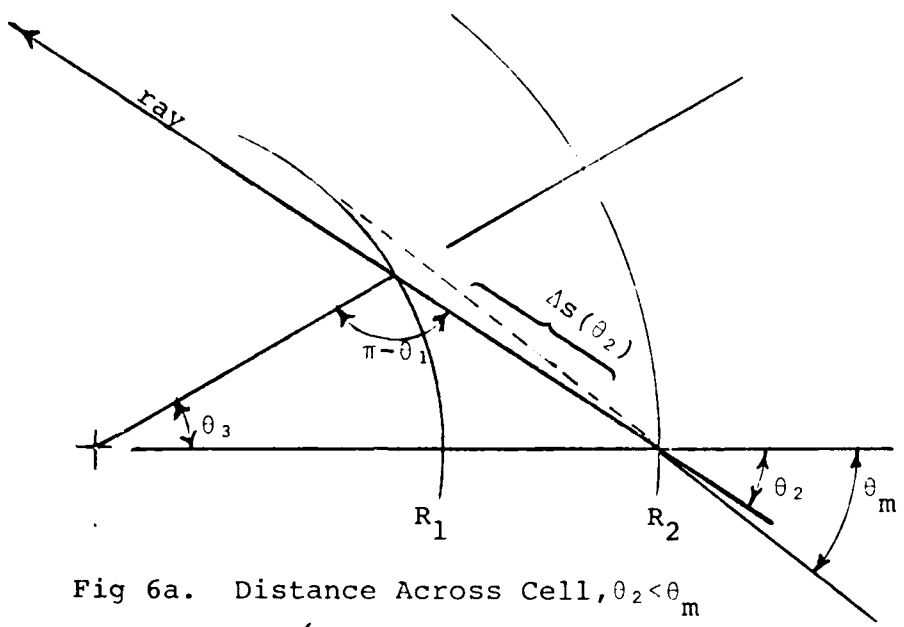


Fig 6a. Distance Across Cell,  $\theta_2 < \theta_m$

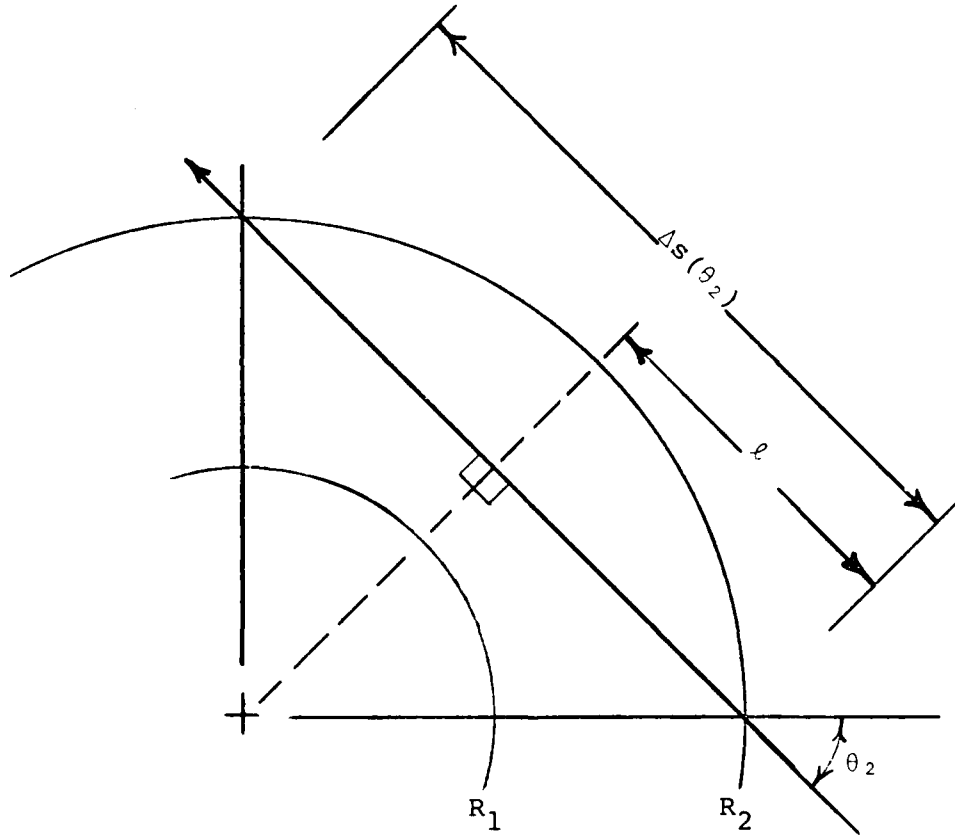


Fig 6b. Distance Across Cell,  $\theta_2 > \theta_m$

$$\theta_3 = \pi - (\pi - \theta_1) - \theta_2 = \theta_1 - \theta_2. \quad (37)$$

By the law of cosines,

$$\Delta s(\theta_2)^2 = R_1^2 + R_2^2 - 2R_1 R_2 \cos(\theta_1 - \theta_2), \quad (38)$$

and using the following identity (Ref 9)

$$\cos(\theta_1 - \theta_2) = \cos\theta_1 \cos\theta_2 + \sin\theta_1 \sin\theta_2. \quad (39)$$

Then

$$\Delta s(\theta_2)^2 = R_1^2 + R_2^2 - 2R_1 R_2 \cos\theta_1 \cos\theta_2 + \sin\theta_1 \sin\theta_2, \quad (40)$$

and since  $\sin^2\theta + \cos^2\theta = 1$ ,

$$\cos\theta_1 = (1 - \sin^2\theta_1)^{\frac{1}{2}} \quad (41)$$

From equation (21),

$$\sin\theta_1 = R_2/R_1 \sin\theta_2, \quad (42)$$

therefore,

$$\cos\theta_1 = (1 - (R_2/R_1)^2 \sin^2\theta_2)^{\frac{1}{2}}, \quad (43)$$

... ,

$$\cos \theta_1 = 1/R_1 (R_1^2 - R_2^2 \sin^2 \theta_2)^{1/2}. \quad (44)$$

now,  $\Delta s(\theta_2)^2$  is,

$$\Delta s(\theta_2)^2 = R_1^2 + R_2^2 - 2R_1 R_2 \{ 1/R_1 (R_1^2 - R_2^2 \sin^2 \theta_2)^{1/2} \cos \theta_2$$

$$+ R_2/R_1 \sin^2 \theta_2 \}$$
 (45)

Combining,

again, since  $\sin^2 \theta + \cos^2 \theta = 1$ ,

$$R_2^2 = R_2^2 (\sin^2 \theta_2 + \cos^2 \theta_2) \quad (47)$$

$$\begin{aligned} \Delta s(\theta_2)^2 &= R_1^2 + R_2^2 \sin^2 \theta_2 + R_2^2 \cos^2 \theta_2 \\ &- 2R_2 (R_1^2 - R_2^2 \sin^2 \theta_2)^{1/2} \cos \theta_2 - 2R_2^2 \sin^2 \theta_2 \end{aligned} \quad (48)$$

$$\begin{aligned} \Delta s(\theta_2)^2 &= R_1^2 - R_2^2 \sin^2 \theta_2 + R_2^2 \cos^2 \theta_2 \\ &- 2R_2 \cos \theta (R_1^2 - R_2^2 \sin^2 \theta_2)^{1/2} \end{aligned} \quad (49)$$

$$\Delta s(\theta_2)^2 = R_2^2 \cos^2 \theta_2 - 2R_2 \cos \theta_2 (R_1^2 - R_2^2 \sin^2 \theta_2)^{\frac{1}{2}} + (R_1^2 - R_2^2 \sin^2 \theta_2) \quad (50)$$

$$\Delta s(\theta_2)^2 = \left\{ R_2 \cos \theta_2 - (R_1^2 - R_2^2 \sin^2 \theta_2)^{\frac{1}{2}} \right\}^2 \quad (51)$$

Therefore

$$\Delta s(\theta_2) = R_2 \cos \theta_2 - (R_1^2 - R_2^2 \sin^2 \theta_2)^{\frac{1}{2}} \quad (52)$$

for  $0 \leq \theta_2 < \theta_m$

For the case where  $\theta_m < \theta_2 \leq \pi/2$ , i.e. a ray enters  $R_2$  at too shallow an angle to enter  $R_1$  before re-emerging through  $R_2$ , then from Fig 6b, it can be seen that

$$\Delta s(\theta_2) = 2l \quad (53)$$

and

$$l = R_2 \cos \theta_2 \quad (54)$$

Therefore

$$\Delta s(\theta_2) = 2R_2 \cos \theta_2 \quad (\theta_m < \theta_2 \leq \pi/2) \quad (55)$$

Zinn assumes that for each frequency group at every point outside the principal radiating sphere, the intensity contribution for a given ray direction has one of two values. If the ray intersects the principal radiating source then the intensity contribution to that point is large. Otherwise the intensity is much less. From any given point, the principal radiating source, called the source from here on, will subtend angle, half of which will be designated  $\theta_s$ . Thus for points exterior to the source, the intensity contributions at a given point will be small for angles  $\theta_s < \theta < \pi$ . See Fig 7. The source radius  $R_s$  must be determined for each frequency group at each timestep.  $R_s$  is defined as the radius at which the optical depth is unity, or

$$1 \geq \sum_1^n \mu_i (R_{i+1} - R_i) \quad (56)$$

and

$$R_s = R_n \quad (57)$$

where  $n$  is the minimum number required to meet the condition in equation (56).

Once  $R_s$  has been determined,  $\theta_s$  is then

$$\theta_s = \sin^{-1} (R_s / R_i) \quad (58)$$

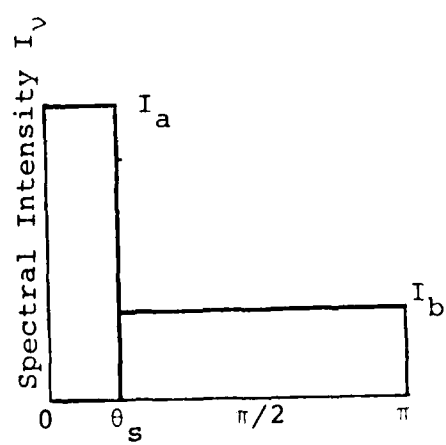
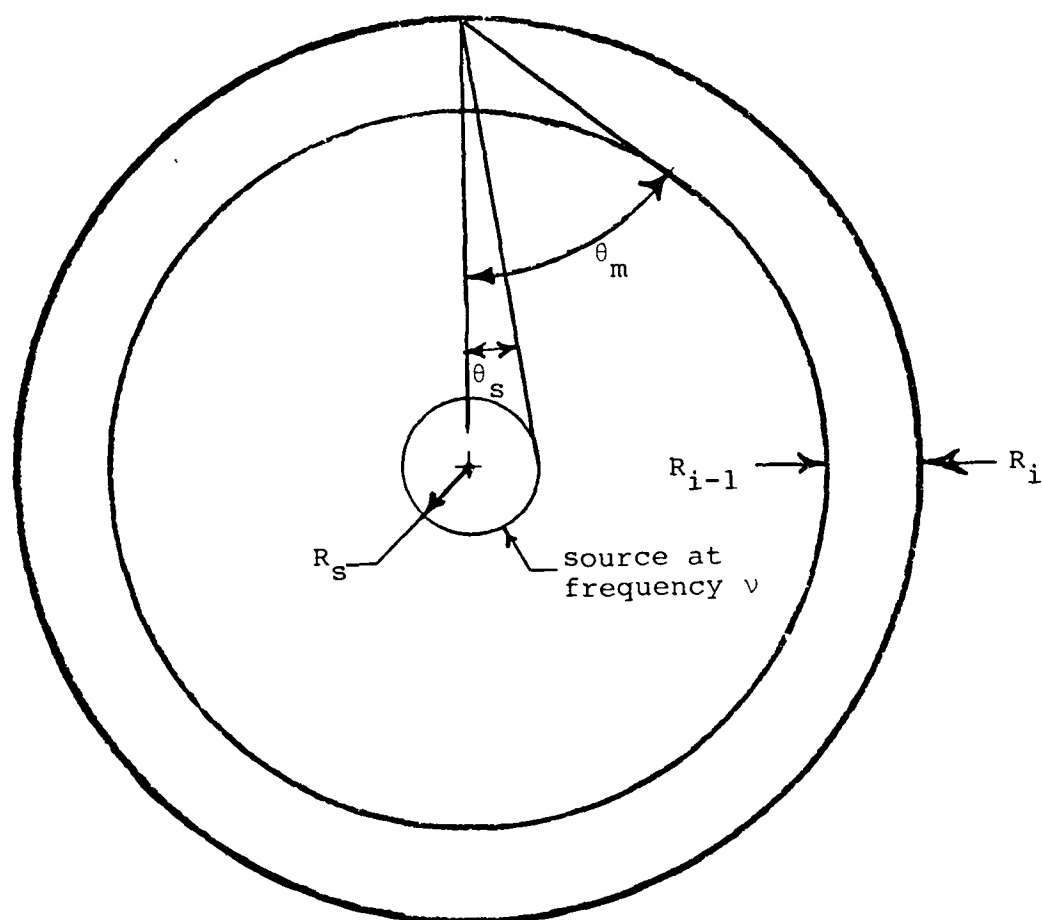


Fig 7. Monochromatic Intensity Distribution

providing  $R_i > R_s$ . If  $R_i < R_s$ , i.e. at a point inside the source, the intensity is then assumed to be isotropic and  $\theta_s$  is set equal to either  $\pi/2$  or to  $\theta_m = \sin^{-1}(R_{i-1}/R_i)$  depending upon whether  $\theta_s$  is being determined as part of the calculation of an inward-going flux.

The assumption that the intensity contribution at each boundary has one of two values ( $I_a$  for  $\theta < \theta_s$ , and  $I_b$  for  $\theta > \theta_s$ ) permits the entire array of fluxes to be generated by just two passes through the mesh (one inward, and one outgoing pass).

"This assumed intensity distribution is exact in two limiting cases; 1) within an optically thick region of uniform temperature region of uniform temperature, where  $I$  does not depend on  $\theta$  (and then  $I_a = I_b$ ), and 2) in a vacuum outside of a uniformly emitting surfaces," (Ref 6).

Now define

$$\theta_{1s} = \begin{cases} \sin^{-1}(R_s/R_1) & \text{for } R_1 > R_s \\ \pi/2 & \text{for } R_1 \leq R_s \end{cases} \quad (59)$$

$$\theta_{2s} = \begin{cases} \sin^{-1}(R_s/R_1) & \text{for } R_1 > R_s \\ \theta_m & \text{for } R_1 \leq R_s \end{cases} \quad (60)$$

Let  $F_1^-$  and  $F_1^+$  be the inward and outward fluxes at  $R_1$  and let  $F_2^-$  and  $F_2^+$  be the inward and outward fluxes at  $R_2$ , (See Fig 8) where  $R_1$  and  $R_2$  are any two adjacent cell boundaries

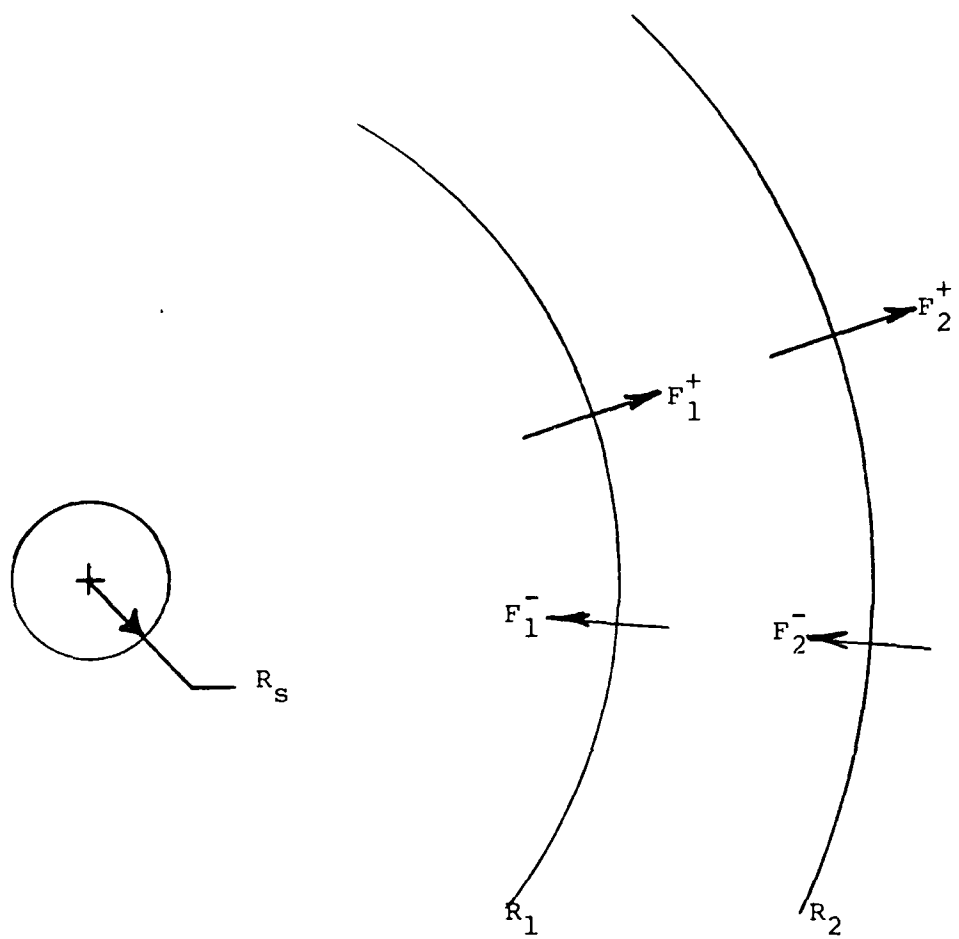


Fig 8. Radiative Transport Labeling Scheme

in the entire mesh such that  $R_2 > R_1$ .

Now using equations (23) and (24) and remembering that  $I_v$  is a constant with one of two values depending on  $\theta$ ,

$$F_v^+ = 2\pi \int_0^{\pi/2} I_v(\theta) \sin\theta \cos\theta d\theta. \quad (23)$$

So,  $F_{1,v}^+$  is

$$F_{1,v}^+ = 2\pi I_{1a} \int_0^{1s} \sin\theta \cos\theta d\theta + 2\pi I_{1b} \int_{1s}^{\pi/2} \sin\theta \cos\theta d\theta, \quad (61)$$

or more simply,

$$F_{1,v}^+ = \pi I_{1a} \sin^2 \theta_{1s} + \pi I_{1b} (1 - \sin^2 \theta_{1s}), \quad (62)$$

$$\text{and } F_{2,v}^+ = 2\pi I_{2a} \int_0^{2s} \sin\theta \cos\theta d\theta + 2\pi I_{2b} \int_{2s}^{\pi/2} \sin\theta \cos\theta d\theta, \quad (63)$$

again simplifying,

$$F_{2,v}^+ = \pi I_{2a} \sin^2 \theta_{2s} + I_{2b} (1 - \sin^2 \theta_{2s}). \quad (64)$$

Starting from equation (24),

$$F_v^- = -2\pi \int_{\pi/2}^{\pi} I_v(\theta) \sin\theta \cos\theta d\theta \quad (24)$$

$F_{1,v}^-$  is

$$F_{1,v}^- = -2\pi I_{1b} \int_{\pi/2}^{\pi} \sin\theta \cos\theta d\theta = I_{1b} \quad (64)$$

and

$$F_{2,v}^- = -2\pi I_{2b} \int_{\pi/2}^{\pi} \sin\theta \cos\theta d\theta = I_{2b} \quad (66)$$

From equation (36),

$$\begin{aligned} F_1^- &= 2\pi/\sin^2\theta_m \int_0^{\theta_m} I_2(\pi-\theta_2) e^{-\mu' \Delta s(\theta_2)} \sin\theta_2 \cos\theta_2 d\theta \\ &+ \pi B \{ 1 - 2/\sin^2\theta_m \int_0^{\theta_m} e^{-\mu' \Delta s(\theta_2)} \sin\theta_2 \cos\theta_2 d\theta_2 \} \quad (36) \end{aligned}$$

$$F_1^- = I_{1b} \quad (67)$$

Equations (62), (64), (66), and (67) result from the two-intensity assumption, and are simplifications of the more exact equations (26) and (36).

The integrals in equations (26) and (36) are all of the form

$$\int_{\theta_A}^{\theta_B} \sin\theta \cos\theta e^{-\mu' \Delta s_1(\theta)} d\theta \quad (68)$$

$$\text{where } \Delta s_1(\theta_2) = R_2 \cos\theta_2 - (R_1^2 - R_2^2 \sin^2\theta_2)^{1/2} \quad (53)$$

or are of the form

$$\int_{\theta_a}^{\theta_b} \sin \theta \cos \theta e^{-\mu' \Delta s(\theta_2)} d\theta \quad (69)$$

where

$$\Delta s(\theta_2) = 2R_2 \cos \theta_2. \quad (55)$$

Both of these integrals can be evaluated in closed form by defining the following:

$$\Delta R \equiv R_2 - R_1 \quad (70)$$

$$\tau \equiv \mu' \Delta R \quad (71)$$

$$u(\theta) = (\tau / \Delta R) (R_2 \cos \theta - (R_1^2 - R_2^2 \sin^2 \theta)^{1/2}) \quad (72)$$

$$u_A = u(\theta_A) \quad (73)$$

$$u_B = u(\theta_B) \quad (74)$$

$$u_s = u(\theta_{2s}) = (\tau / R) ((R_2^2 - R_s^2)^{1/2} - (R_1^2 - R_s^2)^{1/2}) \quad (75)$$

$$u_m = u(\theta_m) = ((R_1 + R_2) / (R_2 - R_1))^{1/2} \tau \quad (76)$$

$$G(u) = e^{-u} (1/u^2 - 1/u) + \int_u^\infty e^{-x} dx \quad (77)$$

$$H(u) = e^{-u} (1 + u) \quad (78)$$

(Equations (72) and (73) are derived in an appendix.)

Then

$$\begin{aligned} \int_{\theta_A}^{\theta_B} \sin\theta \cos\theta e^{-\mu' \Delta s(\theta)} d\theta &= \\ \tau^2 (R_2 + R_1)^2 / (8R_2^2) &\left\{ G(u_A) - G(u_B) \right\} \\ - (R_2 - R_1)^2 / (4R_2^2 \tau^2) &\left\{ H(u_A) - H(u_B) \right\} \end{aligned} \quad (79)$$

and

$$\begin{aligned} \int_{\theta_m}^{\pi/2} \sin\theta \cos\theta e^{-\mu' \Delta s_2(\theta)} d\theta &= \\ (R_2 - R_1)^2 / (4R_2^2 \tau^2) &\left[ 1 - H(2u_m) \right] \end{aligned} \quad (80)$$

Using the above, the equations for the inward-going and outward-going fluxes from a cell as defined by equations (24) and (34) become,

$$F_2^+ = \pi I_{1a} \left\{ (R_1 + R_2) \tau^2 / (4R_2^2) \left\{ G(\tau) - G(u_s) \right\} \right.$$

$$\begin{aligned}
& - (R_2 - R_1)^2 / (2R_2^2 \tau^2) \{ H(z) - H(u_s) \} \Big] \\
& + \pi I_{1b} \left[ (R_1 + R_2)^2 \tau^2 / (4R_2^2) \{ G(u_s) - G(u_m) \} \right] \\
& - \left[ (R_2 - R_1)^2 / (2R_2^2 \tau^2) \{ H(u_s) - H(u_m) \} \right] \\
& + \left[ I_{2b} (R_2 - R_1)^2 / (2R_2^2 \tau^2) \{ 1 - H(2u_m) \} \right] \\
& + \pi B \{ 1 - (R_1 + R_2)^2 \tau^2 / (4R_2^2) \{ G(\tau) - G(u_m) \} \} \\
& - \left[ (R_2 - R_1)^2 / (2R_2^2 \tau^2) \{ 1 - H(\tau) + H(2u_m) \} \right] \quad (81)
\end{aligned}$$

and,

$$\begin{aligned}
F_1^- = & \pi B + \pi (I_{2b} - B) \left[ (R_1 + R_2)^2 \tau^2 / (4R_1^2) \{ G(\tau) - G(u_m) \} \right. \\
& \left. - (R_2 - R_1)^2 / (2R_1^2 \tau^2) \{ H(\tau) - H(u_m) \} \right] \quad (82)
\end{aligned}$$

Next, equations (61), (62), and (63) can be solved for intensities such that

$$I_{1b} = F_1^- / \pi \quad (83)$$

$$I_{2b} = F_2^- / \pi \quad (84)$$

$$I_{1a} = F_1^+ - F_1^- (1 - \sin^2 \theta_{1s}) / \pi \sin^2 \theta_{1s} \quad (85)$$

$$I_{1a} = F_1^+ - F_1^- / \pi \sin^2 \theta_{1s} - F_1^- / \pi \quad (86)$$

Finally, using these equalities, intensities can be eliminated from equation (81) and (82) giving a result using only fluxes. Now,

$$\begin{aligned} F_1^- &= \pi B + (F_2^- - \pi B) \left[ (R_1 + R_2)^2 \tau^2 / (4R_1^2) \{ G(\tau) - G(u_m) \} \right. \\ &\quad \left. - (R_2 - R_1)^2 / (2R_2^2 \tau^2) \{ H(\tau) - H(u_m) \} \right] \end{aligned} \quad (87)$$

and

$$\begin{aligned} F_2^+ &= \pi B + (R_1 + R_2)^2 \tau^2 / (2R_2^2) \left[ (F_1^+ - F_1^-) / \sin^2 \theta_{1s} \{ G(\tau) - G(u_s) \} \right. \\ &\quad \left. + (F_1^- - \pi B) \{ G(u_s) - G(u_m) \} \right] \\ &\quad + (R_2 - R_1)^2 / (2R_2^2 \tau^2) \left[ (F_2^- - \pi B) \{ 1 - H(2u_m) \} \right. \\ &\quad \left. - (F_1^+ - F_1^-) / \sin^2 \theta_{1s} \{ H(\tau) - H(u_s) \} \right. \\ &\quad \left. - (F_1^- - \pi B) \{ H(u_s) - H(u_m) \} \right] \end{aligned} \quad (88)$$

Using equations (84) and (85) it is now possible to compute the entire array of fluxes in just two passes. The flux continuity conditions require

$$F_{1,i+1,v}^+ = F_{2,i,v}^+ \quad (89)$$

and

$$F_{1,i+1,v}^- = F_{2,i,v}^- \quad (90)$$

Starting at the outermost cell with no inward flux ( $F_{1,101,v}^- = 0$ ), equation (87) can be used to compute all of the inward fluxes in terms of the previous flux.

The innermost boundary of the mesh ( $r=0$ ) is a point in spherical geometry, and flux is thru an area, at  $r=0$  both the incoming and outgoing flux is zero. With this boundary fixed, equation (85) can be used to compute all of the outward fluxes using quantities already computed during the current timestep, for the particular frequency group.

Once the array of fluxes has been generated for each frequency group, the rate of change of material energy in a particular cell due to radiation can be determined.

Recall

$$\left. \frac{\partial E_m}{\partial t} \right|_{rad} = - \int_0^\infty \nabla \cdot \vec{F}_v dv \quad (14)$$

where  $\frac{\partial E_m}{\partial t}_{rad}$  is on a per unit volume basis. The volume of any particular cell is:

$$v_i = 4\pi \int_{R_1}^{R_2} r^2 dr \quad (91)$$

therefore the total rate of energy deposition in a given cell is:

$$\frac{\partial E_m}{\partial t}_{rad} \times 4\pi \int_{R_1}^{R_2} r^2 dr = - \int_0^\infty \nabla \cdot F_v dv \cdot \int_{R_1}^{R_2} 4\pi r^2 dr \quad (92)$$

or

$$4\pi/3 (R_2^3 - R_1^3) \frac{\partial E_m}{\partial t}_{rad} = - \int_0^\infty 4\pi \{ R_2^2 (F_2^+ - F_2^-) - R_1^2 (F_2^+ - F_1^-) \} dv \quad (93)$$

Solving for  $\frac{\partial E_m}{\partial t}_{rad}$ ,

$$\frac{\partial E_m}{\partial t}_{rad} = -3/(R_2^3 - R_1^3) \int_0^\infty R_2^2 (F_2^+ - F_2^-) - R_1^2 (F_1^+ - F_1^-) dv \quad (94)$$

Equation (94) governs the transformation of energy into material energy which in turn responds in a manner governed

by the hydrodynamic equations. The hydrodynamic scheme is discussed in the next section, which is followed by a discussion of the radiation and hydrodynamic timestep size in chapter 3.

#### Hydrodynamic Difference Equations

The radiation transport method developed in the last section is used to drive a Lagrangian hydrodynamics scheme. The radiation transport calculations are alternated with the hydro calculations, with one or more hydro sub-steps taken for every radiation timestep. The criteria for determining the sizes of both the radiation timestep and the hydrodynamic timestep are presented in the next chapter.

Two hydro schemes were implemented in RADHOT. Originally, the hydro scheme was the one used in the HUFF code. This hydro scheme is a direct implementation of the equations presented by Richtmeyer and Morton (Ref 2:288-324).

In this scheme, starting with known pressures and constant initial mesh size, the size of the hydrodynamic timestep is computed. Next, the cell boundary velocities and the cell boundary positions are computed. Then, the cell densities, specific volumes and viscous pressure calculated for each cell. The final step is the calculation of the internal energy and pressure of each cell. The finite difference equations to be solved in order are; the cell boundary velocity,

$$u_i^{n+1} = u_i^n + \Delta t_H / \rho (P_{i-1}^n - P_i^n + Q_{i-1}^n - Q_i^n) / \Delta R (R_i^n / R_0)^2, \quad (95)$$

the position of the new cell boundary,

$$R_i^{n+1} = R_i^n + u_i^{n+1} \Delta t_H \quad (96)$$

the specific volume of each cell (and hence the density),

$$v_i^{n+1} = 1/\rho_0 \left[ (R_{i+1}^{n+1})^3 - (R_i^{n+1})^3 / (R_{i+1}^n)^3 - (R_i^n)^3 \right]. \quad (97)$$

If the cell is not expanding then the viscous pressure is,

$$Q_i^{n+1} = 2a^2/v_i^{n+1} + v_i^n (u_{i+1}^{n+1} - u_i^{n+1}), \quad (98)$$

otherwise,

$$Q_i^{n+1} = 0$$

Finally, in the HUFF hydrodynamic scheme, the next two equations are solved iteratively.

$$I_i^{n+1} = I_i^n - \left[ P_i^{n+1} + P_i^n/2 + Q_i^{n+1} \right] (V_i^{n+1} - V_i^n) \quad (99)$$

$$P_i^{n+1} = (\gamma_i - 1) I_i^{n+1} / V_i^{n+1} \quad (100)$$

In the equation above,  $\rho_0$  is the original cell density,  $R_0$  is the original mesh spacing,  $I$  is internal energy, and

" $a$ " is the approximate number of cells over which the shock discontinuity is spread.

In the process of debugging the RADHOT code, the above hydro scheme was dropped in favor of one described by Zinn (Ref 6) in order to more clearly see the coupling between the radiation field and the hydrodynamics it drives. The hydro scheme that Zinn describes for use in conjunction with the transport scheme is apparently also from Richtmeyer and Morton (Ref 2) though it is implemented in such a manner as to avoid the iterative procedure required by the first scheme to determine the internal energy and pressure of each cell. The final hydrodynamic finite difference equations and the sequence that they are to be solved are discussed next.

Initially, the pressures, masses, densities, internal energy, and mesh spacing are determined for time  $t=10^{-7}$  sec. after detonation. All of the energy and weapon mass is placed in the first cell, with all other cells undisturbed from ambient conditions. The hydrodynamic timestep is determined from the Courant conditions, and is required to be equal to or less the limit imposed by radiation considerations.

As the time is incremented from  $t$  to  $t+\Delta t_H$ , the pressure  $P_i$  and the viscous pressure  $Q_i$  for each cell is updated. The pressure,  $P_i$ , is defined by the equation of state and is,

$$P_i = (\gamma_i - 1)\rho_i I_i, \quad (101)$$

and the viscous pressure is,

$$Q_i = \alpha P_i \Delta V_i / c_i \Delta t_H \{ R_i^2 + R_{i+1}^2 \}, \quad (102)$$

where  $\Delta V_i$  is the change in cell volume,  $c$  is the sound speed, and  $\alpha$  is a constant between 0.1 and 1. (fixed at .5 in this thesis). Equation (102) only applies to cells that are not expanding. If a cell is expanding,  $Q_i = 0$ .

"Next, the acceleration  $a_{i+1}$  of each boundary and the displacement of the boundary  $\Delta t_H$  are computed. The internal energy per unit mass for each cell, the cell boundary location  $R_{i+1}$  and the cell boundary velocity,  $v_{i+1}$ , are updated. The difference equations to be applied in sequential order, are:" (Ref 6)

$$a_{i+1} = 8\pi R_{i+1}^2 (P_i + Q_i - P_{i+1} - Q_{i+1}) / (m_i + m_{i+1}) \quad (103)$$

$$\Delta R_{i+1} = \Delta t_H (v_{i+1} + \frac{1}{2} a_{i+1} \Delta t_H), \quad (104)$$

$$I_i = I_i + 4\pi (\rho_i + Q_i) (R_i^2 \Delta R_i - R_{i+1}^2 \Delta R_{i+1}) / m_i \quad (105)$$

$$v_{i+1} = v_{i+1} + a_{i+1} \Delta t_H, \quad (106)$$

and

$$R_{i+1} = R_{i+1} + \Delta R_{i+1} \quad (107)$$

Then the final cell volumes and densities are computed:

$$V_i = 4/3\pi (R_{i+1}^3 - R_i^3) \quad (108)$$

$$\rho_i = m_i/V_i \quad (109)$$

$$\Delta\rho_i = m_i/\Delta V_i \quad (110)$$

Finally, the internal energies  $I_i$  are updated with  $\Delta t_H/\Delta t$  of the radiation energy computed by equation (94) at the beginning of the radiation timestep  $\Delta t$ . Then prior to the next hydro timestep,

$$I_i = I_i + \Delta t_H \left( \frac{\partial E_m}{\partial t} \right)_{rad} / (\Delta\rho_i). \quad (111)$$

at the end of n hydro steps, all of the energy in the  $\left( \frac{\partial E_m}{\partial t} \right)_{rad}$  term will have been dumped into the hydro equations and the next radiation timestep will be taken, beginning the cycle again.

After the above scheme was implemented, it was checked against the HUFF implementation. The two schemes were found to agree to within 10%. The final scheme (Zinn's version) should run faster because it avoids the iteration required in the HUFF scheme.

### III Timestep, Equation of State, and Opacity

#### Timestep Criteria

In the radiation-hydrodynamics scheme described in Chapter II, there are two different timesteps in concurrent use. The first of these is the radiation timestep,  $\Delta t$ . The rate at which radiation energy is being lost to material energy was defined by equation (94). The radiation timestep is chosen such that the fractional change in material energy in any cell in a single timestep does not exceed 10%, or,

$$t = 0.1 \min \left\{ \frac{E_i}{\frac{\partial E}{\partial t}} \right\}_i \quad (112)$$

Zinn notes that this criteria is only useful for problems that are dominated by radiation that is streaming. If the radiation transport is better characterized by the diffusion approximations, then the timestep set by equation (112) becomes very small.

In addition to the radiation timestep, a hydrodynamic timestep is also used. The hydrodynamic timestep,  $\Delta t_H$ , is computed to conform to the stability criteria described by Richtmeyer and Morton (Ref 2). Specifically,

$$1 \geq \frac{c_i t_H}{R_{i+1}^n - R_i^n} \quad (113)$$

where  $c_i$  is the local sound speed and is defined (Ref 10) as,

$$c_i = (\gamma_i p_i / \rho_i)^{\frac{1}{2}} = (\gamma_i (\gamma_i - 1) I_i)^{\frac{1}{2}}. \quad (114)$$

Therefore, combining equations (113) and (114), and remembering that the criteria defined by equation (113) must be met by every cell in the mesh, then the hydrodynamic timestep criteria becomes,

$$\Delta t_H \leq \min \left( \frac{R_{i+1} - R_i}{\left( \frac{\gamma_i p_i}{\rho_i} \right)^{\frac{1}{2}}} \right) \quad (115)$$

The hydrodynamic timestep may not exceed the radiation timestep, although it may be much more limiting. For computational purposes, it is convenient to require that the hydrodynamic timestep be an integral fraction of the radiation timestep so that a fixed amount of the radiation energy can be introduced during each of the hydrodynamic substeps. That is,

$$\Delta t_H = \Delta t/n, \quad n=1, 2, 3, \dots \quad (116)$$

To summarize the difference between the two timesteps, the radiation timestep criteria is set primarily to insure that the Planck function and opacity data are updated frequently enough to accurately compute the radiation fluxes at each cell boundary, and hence accurately determine the amount of material energy being deposited by the radiation field. The hydrodynamic timestep is constrained to ensure sufficient continuity of the material properties of the mesh, and thereby avoiding

local instabilities that would destroy the finite difference scheme's convergence.

#### Equation of State

The equation of state for a gas is,

$$P = (\gamma - 1) \rho I_m \quad (117)$$

where  $P$  is pressure,  $\rho$  is density, and  $I_m$  is internal energy. Gamma,  $\gamma$ , is a variable that ranges from 1.667 for an ideal gas to a low of approximately 1.05 for air at elevated temperatures. At very high temperatures when a gas is fully ionized, gamma will approach the ideal limit. At lower energies, the RADHOT code used a fit to the Nickel-Doan Equation of State for Air (Ref 5) that was developed by Peters for the HUFF code (Ref 4). When a significant fraction of the total energy in a cell is in radiation energy ( $>1\%$ ), then gamma is assumed to be at the ideal limit. This approach turned out to be incorrect, as it results in a discontinuity between the regions where Nickel-Doan applies and the region where the ideal gas approximation is valid. This discontinuity can in turn lead to a splitting of the shock front.

#### Temperature

The temperature of a cell can be determined if the total energy in the cell is known. Specifically,

$$I_{tot} = \frac{3}{2} NkT + \frac{4\sigma}{c} T^4. \quad (118)$$

If the material energy  $I_m$  is known, rather than the total energy, then

$$T = 2I_m / (3Nk) \quad (119)$$

and a time consuming iterative procedure to determine cell temperature is avoided. In equation (119),  $k$  is the Boltzmann constant, and  $N$  is the number of particles in the cell. For the regime of temperatures encompassed by the RADHOT code,  $N$  must be able to adjust from cells in which no ionization has occurred, to cells in which the air molecules are fully ionized, as well as for cells with all intermediate levels of ionization occurring. To do this a fit was suggested by Bridgman (Ref 3) to data reported by Zel'dovich and Raizer (Ref 11). This fit determines the average number of free electrons per atom, as a function of temperature. See Fig 9. Also to be accounted for is the disassociation of molecular nitrogen and oxygen ( $N_2$  and  $O_2$ ) into individual atoms. There are other molecular species in the atmosphere ( $NO$ ,  $CO$ ,  $CO_2$ , etc.) as well as argon, and while some of these species play an important role in determining the opacity of the air, the RADHOT code ignores these other species are in the equation of state. The atmosphere in the RADHOT code is assumed to be 79%  $N_2$  and 21%  $O_2$ . The effective atomic weight of the atmosphere,  $A$ , is assumed to be 14.59 grams/mole. Disassocation of the  $N_2$  and  $O_2$  molecules are assumed to occur at  $20,000^0 K$ ,

which is also the onset of where  $Z^*$  (the number of free electrons per atom) must be included. Therefore if  $T$  is less than  $20,000^0$  K, then,

$$N = \frac{N_0 \rho}{A} \quad (120)$$

In the RADHOT code, a variable  $Q$  is set to either 1 or 2 depending upon whether the temperature is less than or greater than  $20,000^0$  K. From Fig 9,  $Z^*$  was determined to fit the following relation:

$$Z^* = 0 \quad , \quad T \leq 2 \times 10^{4^0} K \quad (122)$$

$$Z^* = 4(\log_{10}T - 4.301), \quad 2 \times 10^{4^0} < T < 10^{6^0} K \quad (123)$$

$$Z^* = 7 \quad , \quad T \geq 10^{6^0} K \quad (124)$$

The temperature then is defined as,

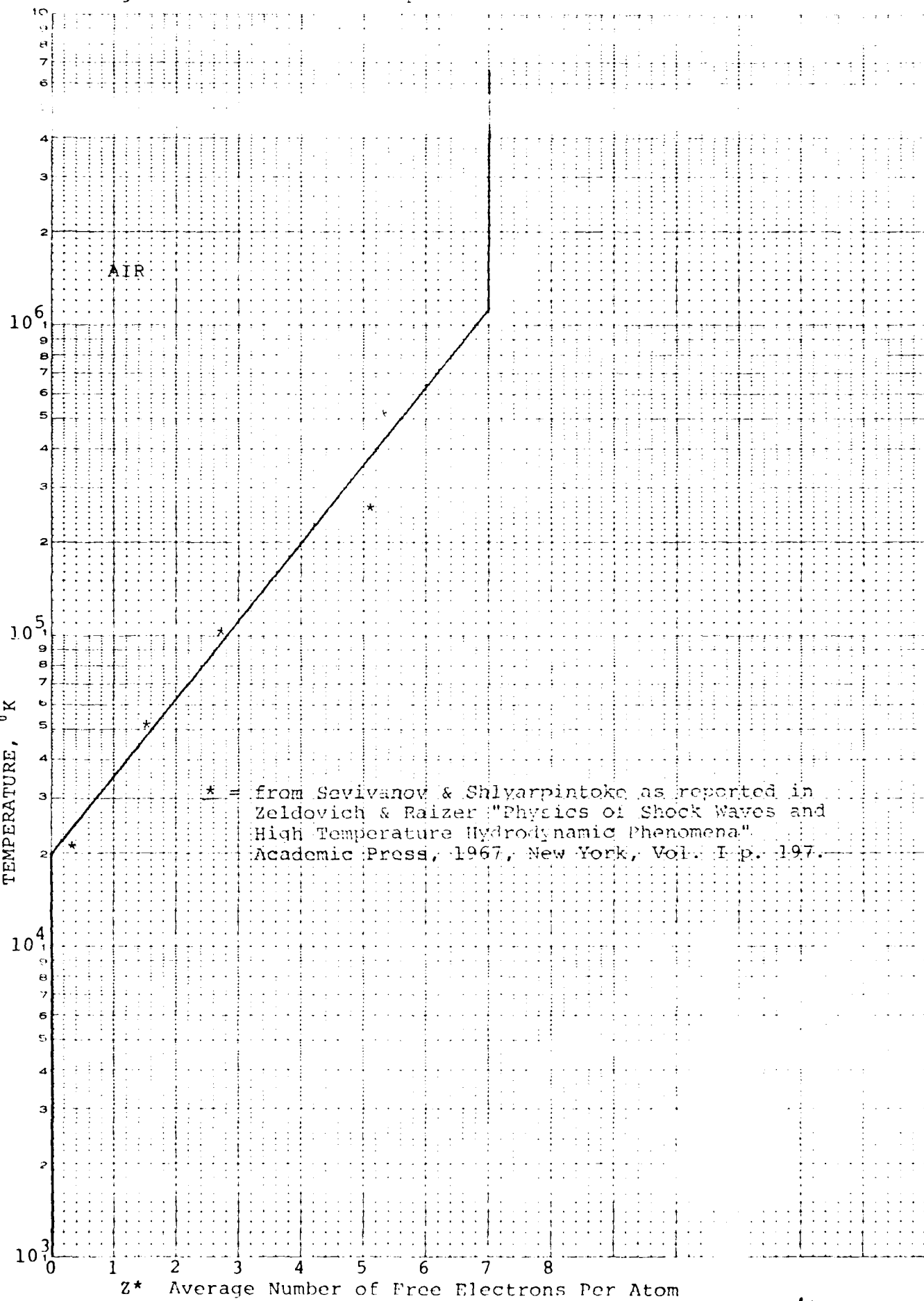
$$T = 2I_m A / [3N_0 \rho Q (Z^* + 1)] . \quad (125)$$

Since  $Q$  and  $Z^*$  are functions of temperature, correct determination of each cell's temperature requires an iterative technique. This proved to be too costly in terms of computer time, so  $Z^*$  and  $Q$  are computed from the old cell temperature

Fig 9. Plot of  $Z^*$  vs Temperature

NO. 340R-L410 DIETZGEN GRAPH PAPER  
SEMI-LOGARITHMIC  
4 CYCLES X 10 DIVISIONS PER INCH

EUGENE DIETZGEN CO.  
MADE IN U. S. A.



first, and then equation (125) is used to compute the current temperature. This method has an inherent error associated with it, but in view of the constraints the timestep criteria places on how rapidly the energy in a cell is allowed to change, the error is considered acceptable.

#### Opacity

Opacity is a measure of the distance that thermal radiation will travel from its source of origin until it is absorbed. In the lower atmosphere, opacity is a complicated function with minor atmospheric constituents playing important roles. Very large computer codes (DANA, DIANE, DIAPHANOUS) have been developed for the accurate prediction of absorption coefficients. These codes are maintained by LASL and the Air Force Weapons Laboratory (AFWL). Opacity data and equation of state data were requested, though never obtained, from AFWL.

Failing to obtain data from AFWL, a fit was made to a graph of absorption coefficients that appeared in Zinn's paper (Ref 6). See Fig 10. The values plotted in Fig 10 are for ambient air density only. When the air density varies from ambient, values obtained from fits to Fig 10 are subject to large (orders of magnitude) errors. Figures 11 and 12 (Ref 12) illustrate this point.

Using fits to Fig 10 data proved unsatisfactory in RADHOT (negative fluxes occasionally resulted), so the absorption coefficients were averaged over frequency, and a smoothly

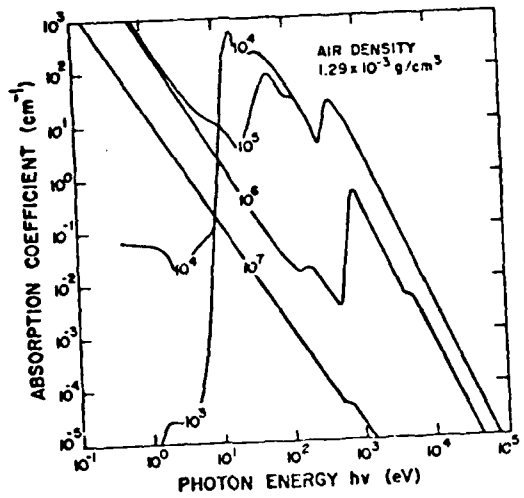


Fig 10. Plots of radiative absorption coefficients vs. photon energy (Ref 6)

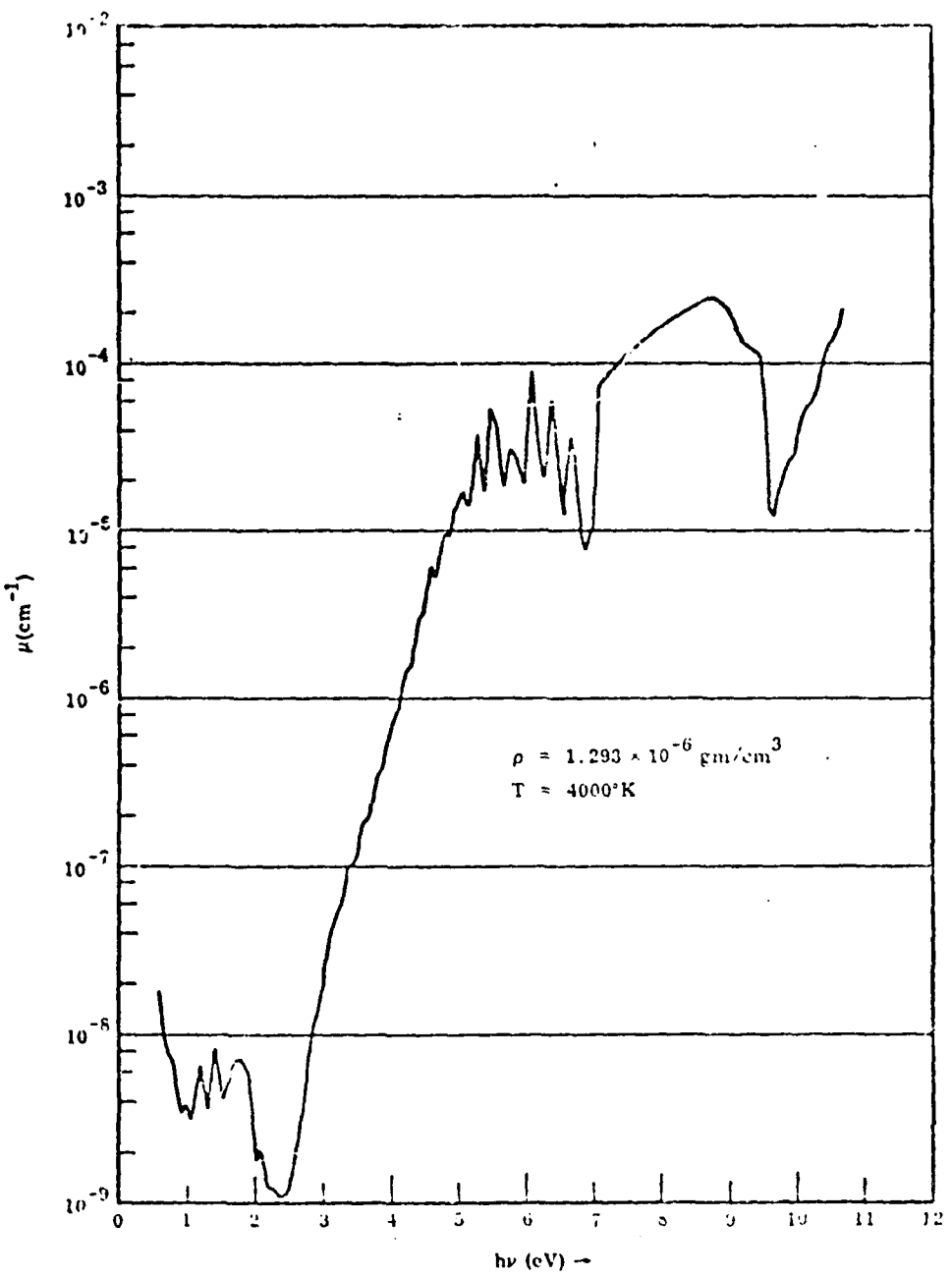


Fig. 11 Absorption Coefficient of Air as a Function of the Photon Energy: Density,  $1.293 \times 10^{-6} \text{ gm/cm}^3$ ; Temperature, 4000 K (Ref 12)

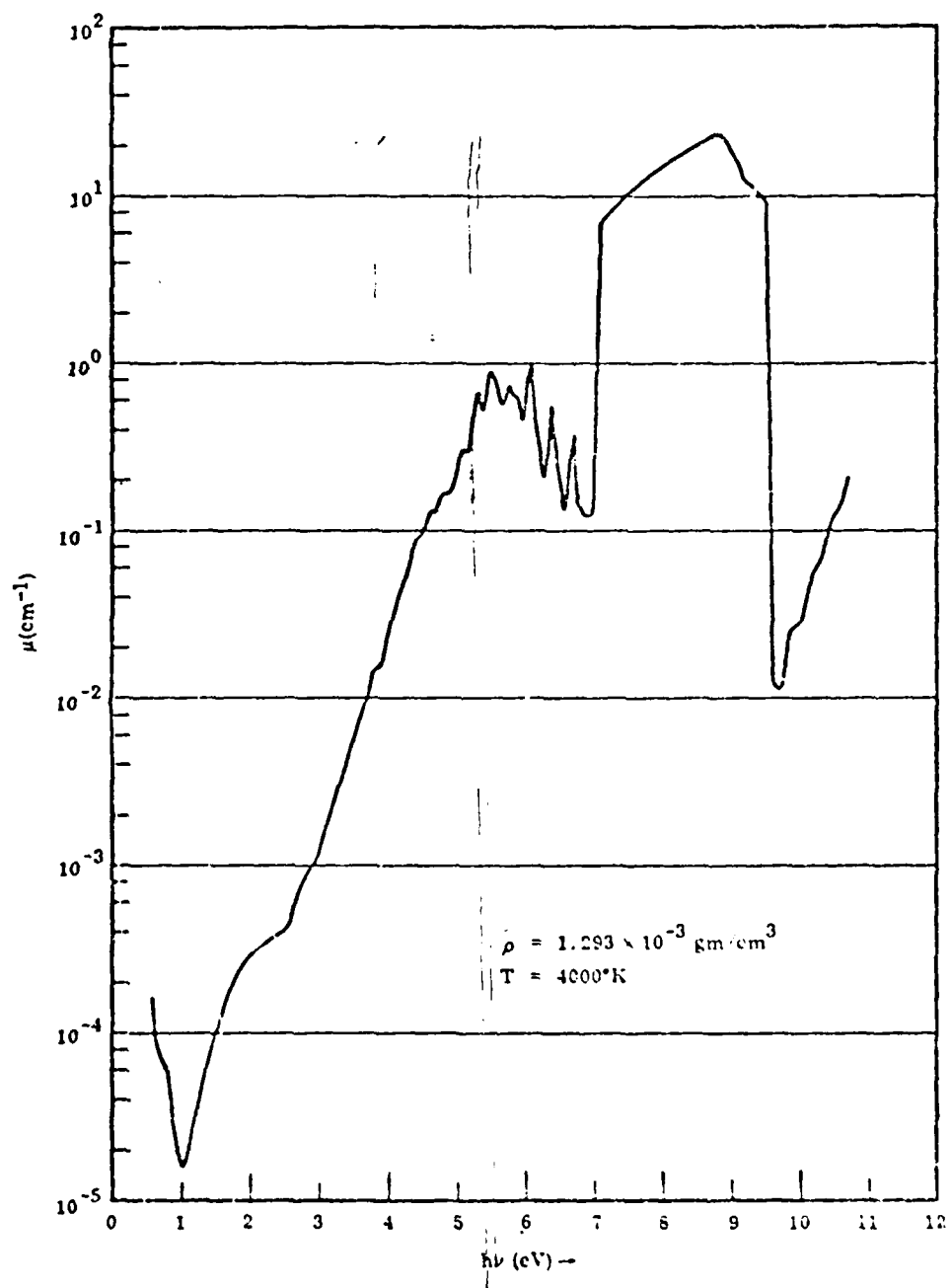


Fig. 12 Absorption Coefficient of Air as a Function of the Photon Energy: Density,  $1.293 \times 10^{-3} \text{ gm/cm}^3$ ; Temperature,  $4000^\circ\text{K}$  (Ref. 12)

varying function of temperature was obtained. Specifically the Rosseland mean is being computed, and it is,

$$(\bar{\mu}')^{-1} = \frac{\int_0^{\infty} \left( \frac{\partial B}{\partial T} \right) \frac{1}{\mu} dv}{\int_0^{\infty} \left( \frac{\partial B}{\partial T} \right) dv} \quad (126)$$

where  $B$  is the Planck function (equation (1)). After  $\bar{\mu}'$  was determined for various temperatures between  $10^{3^0}$  K and  $10^{7^0}$  K, then  $\bar{\mu}'$  can be determined for any temperature in that range by the following relation:

$$\begin{aligned} \ln [\bar{\mu}'(T)^{-1}] &= \ln [\bar{\mu}'(T_i)^{-1}] \left[ \frac{\ln T_{i+1} - \ln T_i}{\ln T_{i+1} - \ln T_i} \right] \\ &+ \ln \bar{\mu}' \left[ (T_{i+1})^{-1} \right] \left[ \frac{\ln T - \ln T_i}{\ln T_{i+1} - \ln T_i} \right] \end{aligned} \quad (127)$$

The Rosseland-averaged absorption coefficient when used in RADHOT no longer predicts negative fluxes, but since the  $\mu'$  used in determining the averages was from Fig 10, variations in density can still result in calculated values of  $\bar{\mu}'$  which may be off by orders of magnitude. This second approach results in the absorption coefficient being strictly a function of temperature. At the high temperatures that are encountered in the innermost cells at the start of the problem, the absorption coefficient forces energy transport to be of a diffusive nature (the cells are optically "thick"). The Rosseland averaging effectively results in the existence of a single frequency

group. With a single frequency group there is no possibility, through absorption and re-radiation, of a portion of the energy in the cell being re-emitted at a frequency where the cell is not optically "thick," and hence continuing the streaming problem. Further discussion of the impact of the lack of valid opacity data on the RADHOT code is in chapter V.

#### IV Problem Definition and Solution

Program RADHOT is designed to solve one-dimensional spherical geometry problems associated with the detonation of a nuclear weapon in the lower atmosphere. The program describes the deposition of thermal radiation energy from the weapon into the surrounding air resulting in the development and propagation of a shock front. The program tracks the temperature, pressure, density, boundary velocity, and viscosity of each of the 100 mesh cells as a function of time, printing out the information for times requested by the user.

Program RADHOT retains the modular programming concepts of its predecessor, HUFF, as well as several subroutines from the original code. The retained subroutines have, in most instances been modified for use in RADHOT. RADHOT is written in FORTRAN IV as implemented on the CDC CYBER series computer.

The radiation hydrodynamics problem is defined by subroutines BLAST and RADSET. The initial conditions are based on the following:

1. The weapon yield is deposited in the first mesh cell, and is divided between a thermal radiation field, and the internal energy deposited in the mass of the first cell.
2. The mass in the first cell is the mass of the weapon, and is arbitrarily fixed at 1000 kg ( $10^6$  grams). The remaining 99 cells in the mesh contain ambient air at a pressure and density adjusted for altitude.
3. The first cell is isothermal.

4. The problem begins at  $10^{-7}$  seconds after detonation (assumed to be the end of the neutronics phase).

Subroutine BLAST is responsible for reading in the weapon yield in KT and altitude scaling factors for different height or burst (HOB). The subroutine scales the programmed values calculating the proper initial conditions for a variety of problems. The altitude scaling parameters provided in Table I are input by the user. The parameters are defined as

$$SP = \frac{P}{P_0} \quad (128)$$

$$SP = \left( \frac{P_0}{P} \right)^{1/3} \quad (129)$$

$$ST = \left( \frac{P_0}{P} \right)^{1/3} \left( \frac{T_0}{T} \right)^{\frac{1}{2}} \quad (130)$$

where  $P_0$  and  $T_0$  are 1.013 dyne-cm<sup>2</sup> and 300°K respectively (Ref 1:104). Subroutine BLAST creates the 100 cell mesh, defining initial cell boundaries, densities, pressures, and cell volumes.

Subroutine RADSET is responsible for further initializing values in the mesh for the radiation transport problem. Subroutine RADSET reads the number of frequency groups to be used and, for every cell except the first one, RADSET determines the mass of air in the cell, and fixes the amount of ambient radiation and material energy in the cell on a per volume basis to a level consistent with a temperature of 300°K. RADSET also fixes the start time of the problem to  $10^{-7}$  sec. For the first mesh cell, RADSET in turn calls another

Table I  
Average Atmospheric Parameters (Ref 1:104)

Altitude (feet)	Scaling Factors			Altitude (feet)	Scaling Factors		
	SP	SD	ST		SP	SD	ST
00	1.00	1.00	1.00	15,000	0.56	1.21	1.28
1,000	0.96	1.01	1.02	20,000	0.46	1.30	1.39
2,000	0.93	1.03	1.03	25,000	0.37	1.39	1.53
3,000	0.90	1.04	1.05	30,000	0.30	1.50	1.68
4,000	0.86	1.05	1.07	35,000	0.24	1.62	1.86
5,000	0.83	1.06	1.08	40,000	0.19	1.75	2.02
10,000	0.69	1.13	1.17				

subroutine, subroutine TEMPO, to determine the temperature and the amount of radiation and material energy in the first cell. Currently, RADFLO's initializing subroutines are fixed to provide information for a one megaton (1MT) weapon, with a weapon mass fixed at 1000 kg. A 1MT weapon results in an initial mesh spacing of 89 cm. Modification to the initializing subroutines (BLAST and RADSET) would be required for problems with different yields and weapon masses.

The RADHOT program is depicted in Fig 13. The program begins by calling subroutines FLAGS. Subroutine FLAGS determines at what times output is requested. RADHOT then transfers control to subroutine CONTROL.

Subroutine CONTROL is responsible for initializing the program, directing the flow of the program and printing the results. Subroutine CONTROL first sets the initial conditions by calling BLAST and RADSET and sets up a loop in which the radiation hydrodynamic calculations are accomplished.

First, subroutine CONTROL calls subroutine Planck which evaluates the Planck function for each cell at each frequency. Then, using opacity data generated by function AMU, the size of the principal radiating source at each frequency is determined. These last two steps generate input that will be required for the radiation transport calculations. Next, the radiation and hydrodynamic timesteps are determined, using criteria presented in chapter III.

Then, subroutine RADFLO is called. Subroutine RADFLO is direct implementation of the radiation transport equations

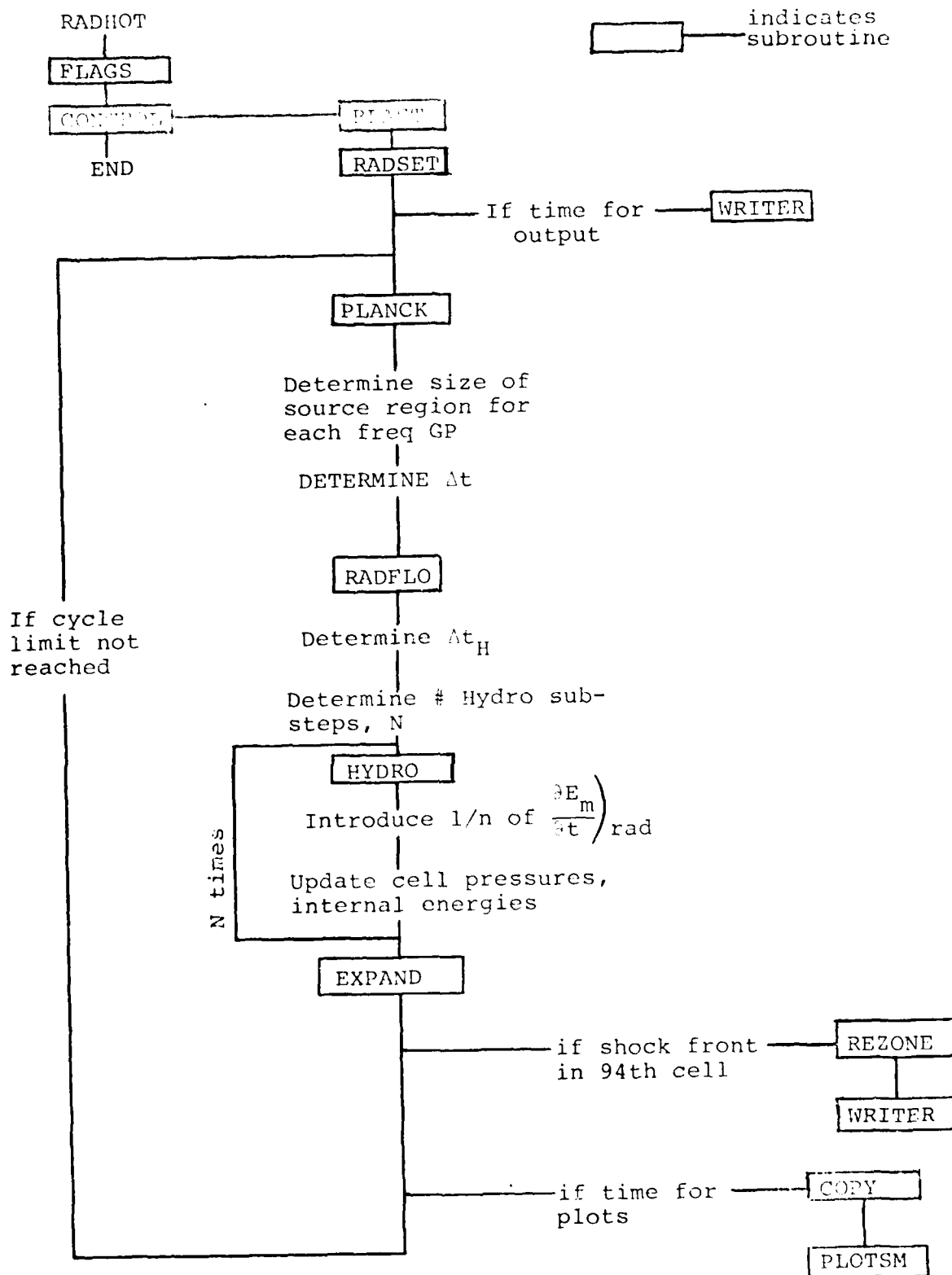


Fig 13. Program RADHOT Flow Diagram

developed in chapter II. Subroutine RADFLO determines the net amount of radiation energy being dumped into material energy in each cell during the current radiation timestep. After RADFLO is executed, subroutine HYDRO is executed one or more times. Subroutine HYDRO implements the second hydro scheme described in chapter II. At the end of each hydrodynamic substep, the internal energy in each cell is updated with the appropriate fraction of the radiation energy being deposited, and the pressure and temperature of each cell is recomputed. Cell temperature is computed in a separate subroutine named TEMPER. Subroutine TEMPER incorporates the Z\* approximation described in chapter III via function ZSTAR.

At the end of each radiation timestep, the elapsed time is updated, and the location of the shock front is identified. If the shock front has reached the 94th cell, then subroutine REZONE is executed and the cell boundaries are relocated in such a manner as to conserve energy. The cell boundaries are moved such that the shock front after re-location is in cell 49.

Finally, prior to continuing on to the next radiation step, a check is made to determine if it is time for printing results. If it is, then subroutine WRITER prints cell parameters (boundaries, pressures, temperatures, densities, radiation and internal energy in the cell, and in-going and out-going fluxes at the cell boundaries. Line printer plots of cell parameters vs position is accomplished by subroutines COPY and PLOTSM.

The program continues cycling until either the time limit or the cycle limit specified by the user (in subroutine FLAGS) is reached.

## V Results and Discussion

Program RADHOT is believed to be "debugged" but is producing reasonable results due to a lack of good, frequency dependent, opacity data, and due to an incomplete equation of state. The equation of state and opacity data currently in the code shows a shock front developing and propagating orders of magnitude slower than expected. The subroutine calculating the absorption coefficient is predicting values in the vicinity of the innermost cells that are far too small. The result is the RADHOT code, which is optimized to handle streaming, is calculating fluxes in a diffusive region.

RADHOT has provisions for treating optically thick cells with diffusion theory, but the code expects that most of the energy transfer thru a cell will be occurring at frequencies where the cell is not optically thick. Unfortunately, the averaging of the absorption coefficients described in chapter III removed the frequency dependence and made the absorption coefficient strictly a function of temperature. The result is that once an optically thick cell is reached, there is no way through absorption and re-emission at a different frequency to stream through that cell. The energy transfer occurring is by diffusion. Zinn, in a code similar to RADHOT, used 40 frequency groups. (Ref 6). RADHOT has provisions in it for up to eight frequency groups, but to the current state of the opacity subroutine, there is no advantage to running more than one group.

Another problem that arises when the code is in a diffusive

regime is that the radiation timestep criteria, equation (112), computes timesteps that are inconveniently small.

During the development of the program, the timestep was noted to grow increasingly smaller as the program progressed. If allowed to run long enough, timesteps of  $10^{-20}$  sec. were eventually generated.

In order to verify that the transport scheme developed in chapter II was working, the portion of the code responsible for diffusion theory calculations was "switched off," and the timestep size was fixed. Doing this shows that the transport code can calculate in a diffusive regime. The shock front slowly propagates outward, and the mesh values remain stable and physically "reasonable," (no negative temperatures, energies, or fluxes and all quantities move in the expected directions as time progresses). Figure 14 is the printout of computed parameters of the first 20 cells for the first two cycles. By the second cycle the second mesh cell is beginning to show the increase in material energy as manifested by a slight increase in cell temperature and pressure. See Fig 14.

At  $7.6 \times 10^{-4}$  sec. after detonation (850 cycles) the rise in temperature and pressure in the second cell are more pronounced, and the DEDT column indicates that energy is beginning to be dumped into the third cell, though the effect is not yet noticeable. See Fig 15. Also at this point in time, the DEDT term shows a very small amount of energy is being deposited in cells 5 and 6. This pair of DEDT terms deta:<sup>h</sup> itself

X	Y	T=40	PRESSURE	DENSITY	EI	DET	F (+)		F (-)	
							E	F	E	F
1	3.4E+012	2.971.97E+014	2.6772E+13	2.1721E+08	5.1631E+15	6.	11572E+13	17.045E+17	6.1721E+14	11572E+13
2	3.1E+012	2.714.35E+012	3.76.1E+7	1.7682E+9	6.121.6E+7	6.	1.1E+2.6E+7	2.77E+5	6.121.6E+7	1.1E+2.6E+7
3	3.2E+012	1.293.1E+012	3.71.5E+7	8.61.07E+7	6.121.1E+7	6.	1.2E+2.9E+7	2.21.9E+7	6.121.1E+7	1.2E+2.9E+7
4	3.3E+012	1.293.3E+012	3.71.1E+7	8.61.07E+7	6.121.1E+7	6.	1.2E+2.9E+7	2.21.9E+7	6.121.1E+7	1.2E+2.9E+7
5	3.4E+012	1.293.5E+012	3.71.6E+7	8.61.07E+7	6.121.6E+7	6.	1.2E+2.9E+7	2.21.9E+7	6.121.6E+7	1.2E+2.9E+7
6	3.5E+012	1.293.7E+012	3.72.1E+7	8.61.07E+7	6.122.1E+7	6.	1.2E+2.9E+7	2.22.4E+7	6.122.1E+7	1.2E+2.9E+7
7	3.6E+012	1.293.9E+012	3.72.6E+7	8.61.07E+7	6.122.6E+7	6.	1.2E+2.9E+7	2.22.9E+7	6.122.6E+7	1.2E+2.9E+7
8	3.7E+012	1.294.1E+012	3.73.1E+7	8.61.07E+7	6.123.1E+7	6.	1.2E+2.9E+7	2.23.4E+7	6.123.1E+7	1.2E+2.9E+7
9	3.8E+012	1.294.3E+012	3.73.6E+7	8.61.07E+7	6.123.6E+7	6.	1.2E+2.9E+7	2.23.9E+7	6.123.6E+7	1.2E+2.9E+7
10	3.9E+012	1.294.5E+012	3.74.1E+7	8.61.07E+7	6.124.1E+7	6.	1.2E+2.9E+7	2.24.4E+7	6.124.1E+7	1.2E+2.9E+7
11	4.0E+012	1.294.7E+012	3.74.6E+7	8.61.07E+7	6.124.6E+7	6.	1.2E+2.9E+7	2.24.9E+7	6.124.6E+7	1.2E+2.9E+7
12	4.1E+012	1.294.9E+012	3.75.1E+7	8.61.07E+7	6.125.1E+7	6.	1.2E+2.9E+7	2.25.4E+7	6.125.1E+7	1.2E+2.9E+7
13	4.2E+012	1.295.1E+012	3.75.6E+7	8.61.07E+7	6.125.6E+7	6.	1.2E+2.9E+7	2.25.9E+7	6.125.6E+7	1.2E+2.9E+7
14	4.3E+012	1.295.3E+012	3.76.1E+7	8.61.07E+7	6.126.1E+7	6.	1.2E+2.9E+7	2.26.4E+7	6.126.1E+7	1.2E+2.9E+7
15	4.4E+012	1.295.5E+012	3.76.6E+7	8.61.07E+7	6.126.6E+7	6.	1.2E+2.9E+7	2.26.9E+7	6.126.6E+7	1.2E+2.9E+7
16	4.5E+012	1.295.7E+012	3.77.1E+7	8.61.07E+7	6.127.1E+7	6.	1.2E+2.9E+7	2.27.4E+7	6.127.1E+7	1.2E+2.9E+7
17	4.6E+012	1.295.9E+012	3.77.6E+7	8.61.07E+7	6.127.6E+7	6.	1.2E+2.9E+7	2.27.9E+7	6.127.6E+7	1.2E+2.9E+7
18	4.7E+012	1.296.1E+012	3.78.1E+7	8.61.07E+7	6.128.1E+7	6.	1.2E+2.9E+7	2.28.4E+7	6.128.1E+7	1.2E+2.9E+7
19	4.8E+012	1.296.3E+012	3.78.6E+7	8.61.07E+7	6.128.6E+7	6.	1.2E+2.9E+7	2.28.9E+7	6.128.6E+7	1.2E+2.9E+7
20	4.9E+012	1.296.5E+012	3.79.1E+7	8.61.07E+7	6.129.1E+7	6.	1.2E+2.9E+7	2.29.4E+7	6.129.1E+7	1.2E+2.9E+7
21	5.0E+012	1.296.7E+012	3.79.6E+7	8.61.07E+7	6.129.6E+7	6.	1.2E+2.9E+7	2.29.9E+7	6.129.6E+7	1.2E+2.9E+7
22	5.1E+012	1.296.9E+012	3.80.1E+7	8.61.07E+7	6.130.1E+7	6.	1.2E+2.9E+7	3.01.2E+7	6.130.1E+7	1.2E+2.9E+7
23	5.2E+012	1.297.1E+012	3.80.6E+7	8.61.07E+7	6.130.6E+7	6.	1.2E+2.9E+7	3.01.7E+7	6.130.6E+7	1.2E+2.9E+7
24	5.3E+012	1.297.3E+012	3.81.1E+7	8.61.07E+7	6.131.1E+7	6.	1.2E+2.9E+7	3.02.2E+7	6.131.1E+7	1.2E+2.9E+7
25	5.4E+012	1.297.5E+012	3.81.6E+7	8.61.07E+7	6.131.6E+7	6.	1.2E+2.9E+7	3.02.7E+7	6.131.6E+7	1.2E+2.9E+7
26	5.5E+012	1.297.7E+012	3.82.1E+7	8.61.07E+7	6.132.1E+7	6.	1.2E+2.9E+7	3.03.2E+7	6.132.1E+7	1.2E+2.9E+7
27	5.6E+012	1.297.9E+012	3.82.6E+7	8.61.07E+7	6.132.6E+7	6.	1.2E+2.9E+7	3.03.7E+7	6.132.6E+7	1.2E+2.9E+7
28	5.7E+012	1.298.1E+012	3.83.1E+7	8.61.07E+7	6.133.1E+7	6.	1.2E+2.9E+7	3.04.2E+7	6.133.1E+7	1.2E+2.9E+7
29	5.8E+012	1.298.3E+012	3.83.6E+7	8.61.07E+7	6.133.6E+7	6.	1.2E+2.9E+7	3.04.7E+7	6.133.6E+7	1.2E+2.9E+7
30	5.9E+012	1.298.5E+012	3.84.1E+7	8.61.07E+7	6.134.1E+7	6.	1.2E+2.9E+7	3.05.2E+7	6.134.1E+7	1.2E+2.9E+7
31	6.0E+012	1.298.7E+012	3.84.6E+7	8.61.07E+7	6.134.6E+7	6.	1.2E+2.9E+7	3.05.7E+7	6.134.6E+7	1.2E+2.9E+7
32	6.1E+012	1.298.9E+012	3.85.1E+7	8.61.07E+7	6.135.1E+7	6.	1.2E+2.9E+7	3.06.2E+7	6.135.1E+7	1.2E+2.9E+7
33	6.2E+012	1.299.1E+012	3.85.6E+7	8.61.07E+7	6.135.6E+7	6.	1.2E+2.9E+7	3.06.7E+7	6.135.6E+7	1.2E+2.9E+7
34	6.3E+012	1.299.3E+012	3.86.1E+7	8.61.07E+7	6.136.1E+7	6.	1.2E+2.9E+7	3.07.2E+7	6.136.1E+7	1.2E+2.9E+7
35	6.4E+012	1.299.5E+012	3.86.6E+7	8.61.07E+7	6.136.6E+7	6.	1.2E+2.9E+7	3.07.7E+7	6.136.6E+7	1.2E+2.9E+7
36	6.5E+012	1.299.7E+012	3.87.1E+7	8.61.07E+7	6.137.1E+7	6.	1.2E+2.9E+7	3.08.2E+7	6.137.1E+7	1.2E+2.9E+7
37	6.6E+012	1.299.9E+012	3.87.6E+7	8.61.07E+7	6.137.6E+7	6.	1.2E+2.9E+7	3.08.7E+7	6.137.6E+7	1.2E+2.9E+7
38	6.7E+012	1.300.1E+012	3.88.1E+7	8.61.07E+7	6.138.1E+7	6.	1.2E+2.9E+7	3.09.2E+7	6.138.1E+7	1.2E+2.9E+7
39	6.8E+012	1.300.3E+012	3.88.6E+7	8.61.07E+7	6.138.6E+7	6.	1.2E+2.9E+7	3.09.7E+7	6.138.6E+7	1.2E+2.9E+7
40	6.9E+012	1.300.5E+012	3.89.1E+7	8.61.07E+7	6.139.1E+7	6.	1.2E+2.9E+7	3.10.2E+7	6.139.1E+7	1.2E+2.9E+7
41	7.0E+012	1.300.7E+012	3.89.6E+7	8.61.07E+7	6.139.6E+7	6.	1.2E+2.9E+7	3.10.7E+7	6.139.6E+7	1.2E+2.9E+7
42	7.1E+012	1.300.9E+012	3.90.1E+7	8.61.07E+7	6.140.1E+7	6.	1.2E+2.9E+7	3.11.2E+7	6.140.1E+7	1.2E+2.9E+7
43	7.2E+012	1.301.1E+012	3.90.6E+7	8.61.07E+7	6.140.6E+7	6.	1.2E+2.9E+7	3.11.7E+7	6.140.6E+7	1.2E+2.9E+7
44	7.3E+012	1.301.3E+012	3.91.1E+7	8.61.07E+7	6.141.1E+7	6.	1.2E+2.9E+7	3.12.2E+7	6.141.1E+7	1.2E+2.9E+7
45	7.4E+012	1.301.5E+012	3.91.6E+7	8.61.07E+7	6.141.6E+7	6.	1.2E+2.9E+7	3.12.7E+7	6.141.6E+7	1.2E+2.9E+7
46	7.5E+012	1.301.7E+012	3.92.1E+7	8.61.07E+7	6.142.1E+7	6.	1.2E+2.9E+7	3.13.2E+7	6.142.1E+7	1.2E+2.9E+7
47	7.6E+012	1.301.9E+012	3.92.6E+7	8.61.07E+7	6.142.6E+7	6.	1.2E+2.9E+7	3.13.7E+7	6.142.6E+7	1.2E+2.9E+7
48	7.7E+012	1.302.1E+012	3.93.1E+7	8.61.07E+7	6.143.1E+7	6.	1.2E+2.9E+7	3.14.2E+7	6.143.1E+7	1.2E+2.9E+7
49	7.8E+012	1.302.3E+012	3.93.6E+7	8.61.07E+7	6.143.6E+7	6.	1.2E+2.9E+7	3.14.7E+7	6.143.6E+7	1.2E+2.9E+7
50	7.9E+012	1.302.5E+012	3.94.1E+7	8.61.07E+7	6.144.1E+7	6.	1.2E+2.9E+7	3.15.2E+7	6.144.1E+7	1.2E+2.9E+7
51	8.0E+012	1.302.7E+012	3.94.6E+7	8.61.07E+7	6.144.6E+7	6.	1.2E+2.9E+7	3.15.7E+7	6.144.6E+7	1.2E+2.9E+7
52	8.1E+012	1.302.9E+012	3.95.1E+7	8.61.07E+7	6.145.1E+7	6.	1.2E+2.9E+7	3.16.2E+7	6.145.1E+7	1.2E+2.9E+7
53	8.2E+012	1.303.1E+012	3.95.6E+7	8.61.07E+7	6.145.6E+7	6.	1.2E+2.9E+7	3.16.7E+7	6.145.6E+7	1.2E+2.9E+7
54	8.3E+012	1.303.3E+012	3.96.1E+7	8.61.07E+7	6.146.1E+7	6.	1.2E+2.9E+7	3.17.2E+7	6.146.1E+7	1.2E+2.9E+7
55	8.4E+012	1.303.5E+012	3.96.6E+7	8.61.07E+7	6.146.6E+7	6.	1.2E+2.9E+7	3.17.7E+7	6.146.6E+7	1.2E+2.9E+7
56	8.5E+012	1.303.7E+012	3.97.1E+7	8.61.07E+7	6.147.1E+7	6.	1.2E+2.9E+7	3.18.2E+7	6.147.1E+7	1.2E+2.9E+7
57	8.6E+012	1.303.9E+012	3.97.6E+7	8.61.07E+7	6.147.6E+7	6.	1.2E+2.9E+7	3.18.7E+7	6.147.6E+7	1.2E+2.9E+7
58	8.7E+012	1.304.1E+012	3.98.1E+7	8.61.07E+7	6.148.1E+7	6.	1.2E+2.9E+7	3.19.2E+7	6.148.1E+7	1.2E+2.9E+7
59	8.8E+012	1.304.3E+012	3.98.6E+7	8.61.07E+7	6.148.6E+7	6.	1.2E+2.9E+7	3.19.7E+7	6.148.6E+7	1.2E+2.9E+7
60	8.9E+012	1.304.5E+012	3.99.1E+7	8.61.07E+7	6.149.1E+7	6.	1.2E+2.9E+7	3.20.2E+7	6.149.1E+7	1.2E+2.9E+7
61	9.0E+012	1.304.7E+012	3.99.6E+7	8.61.07E+7	6.149.6E+7	6.	1.2E+2.9E+7	3.20.7E+7	6.149.6E+7	1.2E+2.9E+7
62	9.1E+012	1.304.9E+012	4.00.1E+7	8.61.07E+7	6.150.1E+7	6.	1.2E+2.9E+7	3.21.2E+7	6.150.1E+7	1.2E+2.9E+7
63	9.2E+012	1.305.1E+012	4.00.6E+7	8.61.07E+7	6.150.6E+7	6.	1.2E+2.9E+7	3.21.7E+7	6.150.6E+7	1.2E+2.9E+7
64	9.3E+012	1.305.3E+012	4.01.1E+7	8.61.07E+7	6.151.1E+7	6.	1.2E+2.9E+7	3.22.2E+7	6.151.1E+7	1.2E+2.9E+7
65	9.4E+012	1.305.5E+012	4.01.6E+7	8.61.07E+7	6.151.6E+7	6.	1.2E+2.9E+7	3.22.7E+7	6.151.6E+7	1.2E+2.9E+7
66	9.5E+012	1.305.7E+012	4.02.1E+7	8.61.07E+7	6.152.1E+7	6.	1.2E+2.9E+7	3.23.2E+7	6.152.1E+7	1.2E+2.9E+7
67	9.6E+012	1.305.9E+012	4.02.6E+7	8.61.07E+7	6.152.6E+7	6.	1.2E+2.9E+7	3.23.7E+7	6.152.6E+7	1.2E+2.9E+7
68	9.7E+012	1.306.1E+012	4.03.1E+7	8.61.07E+7	6.153.1E+7	6.	1.2E+2.9E+7	3.24.2E+7	6.153.1E+7	1.2E+2.9E+7
69	9.8E+012	1.306.3E+012	4.03.6E+7	8.61.07E+7	6.153.6E+7	6.	1.2E+2.9E+7	3.24.7E+7	6.153.6E+7	1.2E+2.9E+7
70	9.9E+012	1.306.5E+012	4.04.1E+7	8.61.07E+7	6.154.1E+7	6.	1.2E+2.9E+7	3.2		

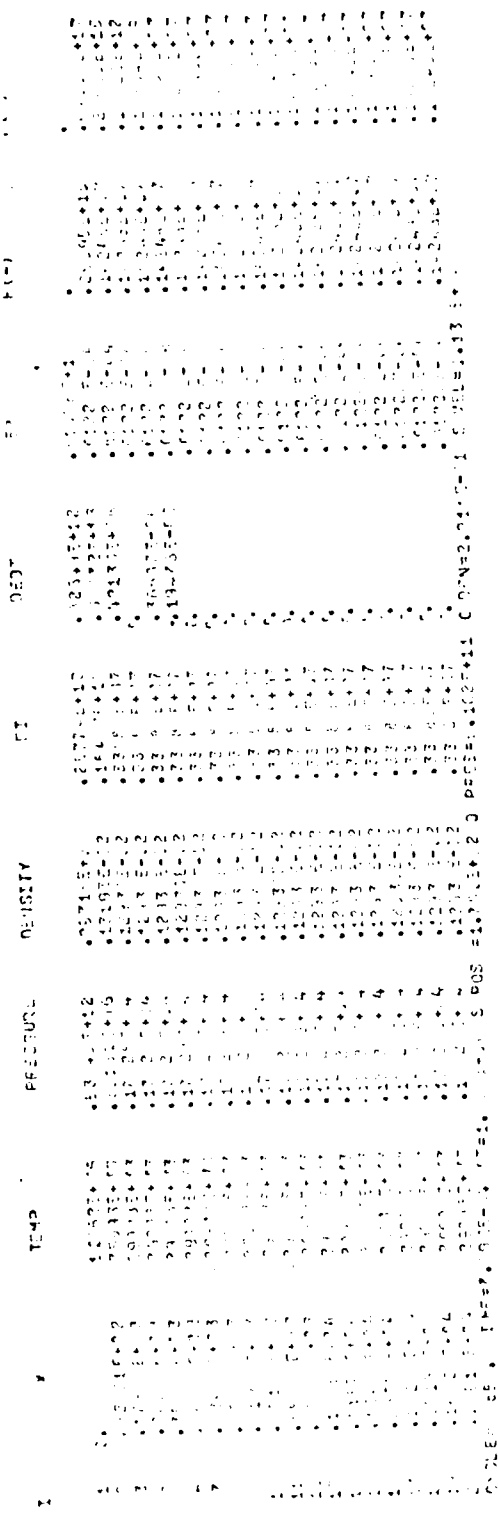


Fig 15. LMT BLAST,  $7.6 \times 10^{-4}$  sec.

from the principle radiating source and travels rapidly through the mesh. This phenomena occurs at random intervals during the program run. This may be the "shock splitting" mentioned in chapter III, arising due to the discontinuity in the equation of state, or it may merely be a computational anomaly.

By  $2.7 \times 10^{-3}$  sec. after detonation (cycle 2800), the first two cells are beginning to come into equilibrium with each other. Also the boundary between the first and second cell is beginning to expand outward, compressing the air in the second cell. See Fig 16. Finally, by  $4.5 \times 10^{-3}$  sec. (cycle 4600) the first two cells are nearly in equilibrium with each other and the third cell continues to heat up. See Fig 17. The reason, in part, for the slowing of the shock front is that though each concentric shell has approximately the same thickness, the total amount of mass of air in each shell increases with radial distance from the source.

Due to the amount of CPU time required to run RADHOT, the problem has not been run beyond 4600 cycles. Also, the above run was for a single frequency group. RADHOT required 800 seconds of CP time to run 4600 cycles, or roughly 0.18 seconds per cycle. Running with more than one frequency group, as would be required to do the problem properly, would further worsen the situation. Further work on RADHOT will, in addition to improving the opacity data, have to look at ways of decreasing the cycle time. RADHOT does not, however require large amounts of memory, approximately 68,000 memory locations.

T	X	TEMP	PRESSURE	DENSITY	EI	DEDT	EP	F(-)	F(+)
1	0.	1.5951E+18	1.9971E+11	1.9332E+32	1.3719E+13	2.9873E+10	5.1854E+15	6.	5.1572E+9
2	1.2986E+18	1.9315E+65	1.9315E+65	1.9315E+65	1.3551E+13	2.135E+10	2.135E+10	6.	5.1563E+44
3	1.6875E+18	2.13E+65	1.7128E+64	1.2233E+62	1.3551E+13	2.135E+10	2.135E+10	6.	7.35E+14
4	2.770CE+18	2.97E+63	1.1729E+63	1.2935E+62	3.716E+12	6.1221E+7	6.1221E+7	6.	1.57E+62
5	3.515E+18	3.93E+63	1.1934E+63	1.2935E+62	3.716E+12	6.1221E+7	6.1221E+7	6.	1.57E+62
6	4.651E+18	4.97E+62	1.1728E+64	1.2233E+62	3.716E+12	6.1221E+7	6.1221E+7	6.	1.57E+62
7	5.744E+18	5.97E+62	1.1934E+63	1.2233E+62	3.716E+12	6.1221E+7	6.1221E+7	6.	1.57E+62
8	6.744E+18	6.97E+62	1.1728E+64	1.2233E+62	3.716E+12	6.1221E+7	6.1221E+7	6.	1.57E+62
9	7.744E+18	7.97E+62	1.1934E+63	1.2233E+62	3.716E+12	6.1221E+7	6.1221E+7	6.	1.57E+62
10	8.744E+18	8.97E+62	1.1728E+64	1.2233E+62	3.716E+12	6.1221E+7	6.1221E+7	6.	1.57E+62
11	9.744E+18	9.97E+62	1.1934E+63	1.2233E+62	3.716E+12	6.1221E+7	6.1221E+7	6.	1.57E+62
12	1.074E+19	1.97E+62	1.1728E+64	1.2233E+62	3.716E+12	6.1221E+7	6.1221E+7	6.	1.57E+62
13	1.174E+19	2.97E+62	1.1934E+63	1.2233E+62	3.716E+12	6.1221E+7	6.1221E+7	6.	1.57E+62
14	1.274E+19	3.97E+62	1.1728E+64	1.2233E+62	3.716E+12	6.1221E+7	6.1221E+7	6.	1.57E+62
15	1.374E+19	4.97E+62	1.1934E+63	1.2233E+62	3.716E+12	6.1221E+7	6.1221E+7	6.	1.57E+62
16	1.474E+19	5.97E+62	1.1728E+64	1.2233E+62	3.716E+12	6.1221E+7	6.1221E+7	6.	1.57E+62
17	1.574E+19	6.97E+62	1.1934E+63	1.2233E+62	3.716E+12	6.1221E+7	6.1221E+7	6.	1.57E+62
18	1.674E+19	7.97E+62	1.1728E+64	1.2233E+62	3.716E+12	6.1221E+7	6.1221E+7	6.	1.57E+62
19	1.774E+19	8.97E+62	1.1934E+63	1.2233E+62	3.716E+12	6.1221E+7	6.1221E+7	6.	1.57E+62
20	1.874E+19	9.97E+62	1.1728E+64	1.2233E+62	3.716E+12	6.1221E+7	6.1221E+7	6.	1.57E+62
CYCLE= 23., * TXTE=2.7.9E-3 DT=1.0.1E-15 S POS =1.7.81E+12 J RES=6.563J+1R 0 DEN=1.0E-11 S V-L=2.377E+14									

Fig 16. 1MT BLAST,  $2.7 \times 10^{-3}$  sec.

<i>T</i>	<i>X</i>	<i>Y</i>	TEMP	PRESSURE	DENSITY	F(+)	F(-)
1	1.985	3.2E+06	• 22679 E+11	• 445 E+22 -• 21	• 735598 E+42	• 1187 E+42	• 51072 E+15
2	1.712	3.2E+03	• 16144 E+5	• 22235 E+11	• 1133 E+14	• 3983 E+12	• 6622 E+14
3	1.786	3.2E+03	• 21513 E+5	• 12933 E+11	• 32121 E+12	• 21613 E+12	• 15732 E+12
4	2.577	3.2E+03	• 21504 E+5	• 17285 E+11	• 12332 E+12	• 21761 E+12	• 13724 E+12
5	3.782	3.2E+03	• 23692 E+5	• 17285 E+11	• 12332 E+12	• 21761 E+12	• 13724 E+12
6	4.451	3.2E+03	• 24935 E+5	• 12933 E+11	• 12332 E+12	• 21761 E+12	• 13724 E+12
7	5.246	3.2E+03	• 17233 E+4	• 12933 E+11	• 32121 E+12	• 12332 E+12	• 12332 E+12
8	6.212	3.2E+03	• 21513 E+4	• 12933 E+11	• 32121 E+12	• 12332 E+12	• 12332 E+12
9	7.357	3.2E+03	• 21504 E+4	• 12933 E+11	• 32121 E+12	• 12332 E+12	• 12332 E+12
10	8.672	3.2E+03	• 21504 E+4	• 12933 E+11	• 32121 E+12	• 12332 E+12	• 12332 E+12
11	10.164	3.2E+03	• 21504 E+4	• 12933 E+11	• 32121 E+12	• 12332 E+12	• 12332 E+12
12	11.734	3.2E+03	• 21504 E+4	• 12933 E+11	• 32121 E+12	• 12332 E+12	• 12332 E+12
13	13.4	3.2E+03	• 21504 E+4	• 12933 E+11	• 32121 E+12	• 12332 E+12	• 12332 E+12
14	15.2	3.2E+03	• 21504 E+4	• 12933 E+11	• 32121 E+12	• 12332 E+12	• 12332 E+12
15	17.1	3.2E+03	• 21504 E+4	• 12933 E+11	• 32121 E+12	• 12332 E+12	• 12332 E+12
16	19.1	3.2E+03	• 21504 E+4	• 12933 E+11	• 32121 E+12	• 12332 E+12	• 12332 E+12
17	21.2	3.2E+03	• 21504 E+4	• 12933 E+11	• 32121 E+12	• 12332 E+12	• 12332 E+12
18	23.4	3.2E+03	• 21504 E+4	• 12933 E+11	• 32121 E+12	• 12332 E+12	• 12332 E+12
19	25.7	3.2E+03	• 21504 E+4	• 12933 E+11	• 32121 E+12	• 12332 E+12	• 12332 E+12
C.	27.1	3.2E+03	• 21504 E+4	• 12933 E+11	• 32121 E+12	• 12332 E+12	• 12332 E+12

Fig 17. 1MT BLAST, 4.5 x 10<sup>-3</sup> sec.

Finally, one further check was made to check the functioning of the program. The opacity was fixed at  $10^{-3} \text{ cm}^{-1}$  throughout the run. The results are shown in figures 18 and 19.

By the second cycle, energy is streaming strongly outward as denoted by the F(+) column. The outward flux falls off roughly as  $1/R^2$ . By cycle 850 energy is still flowing through the mesh as denoted by the DEDT terms. The temperature of the innermost cell is lower than in the previous example, and this is due to the energy that was lost when it streamed to be deposited in cells further out. This result is what would be expected if the code was running properly, but contained bad opacity and equation of state information.

IRRADIATION EFFECTS HAVE BEEN INCONSIDERED AT 54 TIMES

CELESTE FORMS SENT IN

$$2.6 \cdot 10^{-3} = \frac{1}{5 \cdot 9 \cdot 10^{-6} - 3} \quad 3.0 \cdot 10^{-3} = \frac{1}{9 \cdot 10^{-6} - 2} \quad 8.0 \cdot 10^{-3} = \frac{1}{8 \cdot 10^{-6} - 1}$$

THE XMAS CARD IS FOR THE CHILDREN OF THE CAMP.

$\mu$	$\mu_{\text{F}}$	$\mu_{\text{S}}$	$\mu_{\text{F}} - \mu_{\text{S}}$	$\mu_{\text{F}}$	$\mu_{\text{S}}$	$\mu_{\text{F}} - \mu_{\text{S}}$	$\mu_{\text{F}}$	$\mu_{\text{S}}$	$\mu_{\text{F}} - \mu_{\text{S}}$
-1.0	-1.0	-1.0	0.0	-1.0	-1.0	0.0	-1.0	-1.0	0.0
-0.9	-0.9	-0.9	0.0	-0.9	-0.9	0.0	-0.9	-0.9	0.0
-0.8	-0.8	-0.8	0.0	-0.8	-0.8	0.0	-0.8	-0.8	0.0
-0.7	-0.7	-0.7	0.0	-0.7	-0.7	0.0	-0.7	-0.7	0.0
-0.6	-0.6	-0.6	0.0	-0.6	-0.6	0.0	-0.6	-0.6	0.0
-0.5	-0.5	-0.5	0.0	-0.5	-0.5	0.0	-0.5	-0.5	0.0
-0.4	-0.4	-0.4	0.0	-0.4	-0.4	0.0	-0.4	-0.4	0.0
-0.3	-0.3	-0.3	0.0	-0.3	-0.3	0.0	-0.3	-0.3	0.0
-0.2	-0.2	-0.2	0.0	-0.2	-0.2	0.0	-0.2	-0.2	0.0
-0.1	-0.1	-0.1	0.0	-0.1	-0.1	0.0	-0.1	-0.1	0.0
0.0	0.0	0.0	0.0	0.0	0.0	0.0	0.0	0.0	0.0
0.1	0.1	0.1	0.0	0.1	0.1	0.0	0.1	0.1	0.0
0.2	0.2	0.2	0.0	0.2	0.2	0.0	0.2	0.2	0.0
0.3	0.3	0.3	0.0	0.3	0.3	0.0	0.3	0.3	0.0
0.4	0.4	0.4	0.0	0.4	0.4	0.0	0.4	0.4	0.0
0.5	0.5	0.5	0.0	0.5	0.5	0.0	0.5	0.5	0.0
0.6	0.6	0.6	0.0	0.6	0.6	0.0	0.6	0.6	0.0
0.7	0.7	0.7	0.0	0.7	0.7	0.0	0.7	0.7	0.0
0.8	0.8	0.8	0.0	0.8	0.8	0.0	0.8	0.8	0.0
0.9	0.9	0.9	0.0	0.9	0.9	0.0	0.9	0.9	0.0
1.0	1.0	1.0	0.0	1.0	1.0	0.0	1.0	1.0	0.0

<i>X</i>	<i>T<sub>0</sub></i>	PRESSURE	DENSITY	EI	DEOT	ER	F(+)	F(-)
1.0	1.0	2.9735E+12	2.57723E+12	2.57723E+12	352.47E+11	53974.5E+15	25.5945E+15	3.365E+15
1.2	1.2	1.71325E+12	2.2175E+12	2.2175E+12	379.65E+11	622.5E-4	1.274.5E+15	1.274.5E+15
1.4	1.4	9.5425E+11	1.42325E+12	1.42325E+12	371.18E+11	6172.5E-4	1.274.5E+15	1.274.5E+15
1.6	1.6	5.296E+11	1.1377E+12	1.1377E+12	41.13E+12	6122.5E-4	1.274.5E+15	1.274.5E+15
1.8	1.8	3.093E+11	1.2933E+12	1.2933E+12	46.87E+12	6122.5E-4	1.274.5E+15	1.274.5E+15
2.0	2.0	1.853E+11	1.2033E+12	1.2033E+12	52.47E+12	6122.5E-4	1.274.5E+15	1.274.5E+15
2.2	2.2	1.153E+11	1.1233E+12	1.1233E+12	57.97E+12	6122.5E-4	1.274.5E+15	1.274.5E+15
2.4	2.4	7.533E+10	1.0433E+12	1.0433E+12	63.37E+12	6122.5E-4	1.274.5E+15	1.274.5E+15
2.6	2.6	4.923E+10	9.533E+11	9.533E+11	68.67E+12	6122.5E-4	1.274.5E+15	1.274.5E+15
2.8	2.8	3.213E+10	8.633E+11	8.633E+11	74.87E+12	6122.5E-4	1.274.5E+15	1.274.5E+15
3.0	3.0	2.093E+10	7.733E+11	7.733E+11	81.07E+12	6122.5E-4	1.274.5E+15	1.274.5E+15
3.2	3.2	1.353E+10	6.8533E+11	6.8533E+11	87.27E+12	6122.5E-4	1.274.5E+15	1.274.5E+15
3.4	3.4	9.023E+09	5.9733E+11	5.9733E+11	93.47E+12	6122.5E-4	1.274.5E+15	1.274.5E+15
3.6	3.6	6.013E+09	5.1933E+11	5.1933E+11	99.67E+12	6122.5E-4	1.274.5E+15	1.274.5E+15
3.8	3.8	4.203E+09	4.4133E+11	4.4133E+11	105.87E+12	6122.5E-4	1.274.5E+15	1.274.5E+15
4.0	4.0	3.003E+09	3.6333E+11	3.6333E+11	112.07E+12	6122.5E-4	1.274.5E+15	1.274.5E+15
4.2	4.2	2.203E+09	2.8533E+11	2.8533E+11	118.27E+12	6122.5E-4	1.274.5E+15	1.274.5E+15
4.4	4.4	1.603E+09	2.0733E+11	2.0733E+11	124.47E+12	6122.5E-4	1.274.5E+15	1.274.5E+15
4.6	4.6	1.143E+09	1.2933E+11	1.2933E+11	130.67E+12	6122.5E-4	1.274.5E+15	1.274.5E+15
4.8	4.8	8.203E+08	5.1933E+10	5.1933E+10	136.87E+12	6122.5E-4	1.274.5E+15	1.274.5E+15
5.0	5.0	6.003E+08	3.6333E+10	3.6333E+10	143.07E+12	6122.5E-4	1.274.5E+15	1.274.5E+15
5.2	5.2	4.403E+08	2.0733E+10	2.0733E+10	149.27E+12	6122.5E-4	1.274.5E+15	1.274.5E+15
5.4	5.4	3.203E+08	1.2933E+10	1.2933E+10	155.47E+12	6122.5E-4	1.274.5E+15	1.274.5E+15
5.6	5.6	2.203E+08	5.1933E+09	5.1933E+09	161.67E+12	6122.5E-4	1.274.5E+15	1.274.5E+15
5.8	5.8	1.603E+08	3.6333E+09	3.6333E+09	167.87E+12	6122.5E-4	1.274.5E+15	1.274.5E+15
6.0	6.0	1.143E+08	2.0733E+09	2.0733E+09	174.07E+12	6122.5E-4	1.274.5E+15	1.274.5E+15
6.2	6.2	8.203E+07	1.2933E+09	1.2933E+09	180.27E+12	6122.5E-4	1.274.5E+15	1.274.5E+15
6.4	6.4	6.003E+07	5.1933E+08	5.1933E+08	186.47E+12	6122.5E-4	1.274.5E+15	1.274.5E+15
6.6	6.6	4.403E+07	3.6333E+08	3.6333E+08	192.67E+12	6122.5E-4	1.274.5E+15	1.274.5E+15
6.8	6.8	3.203E+07	2.0733E+08	2.0733E+08	198.87E+12	6122.5E-4	1.274.5E+15	1.274.5E+15
7.0	7.0	2.203E+07	1.2933E+08	1.2933E+08	205.07E+12	6122.5E-4	1.274.5E+15	1.274.5E+15
7.2	7.2	1.603E+07	5.1933E+07	5.1933E+07	211.27E+12	6122.5E-4	1.274.5E+15	1.274.5E+15
7.4	7.4	1.143E+07	3.6333E+07	3.6333E+07	217.47E+12	6122.5E-4	1.274.5E+15	1.274.5E+15
7.6	7.6	8.203E+06	2.0733E+07	2.0733E+07	223.67E+12	6122.5E-4	1.274.5E+15	1.274.5E+15
7.8	7.8	6.003E+06	1.2933E+07	1.2933E+07	229.87E+12	6122.5E-4	1.274.5E+15	1.274.5E+15
8.0	8.0	4.403E+06	5.1933E+06	5.1933E+06	236.07E+12	6122.5E-4	1.274.5E+15	1.274.5E+15
8.2	8.2	3.203E+06	3.6333E+06	3.6333E+06	242.27E+12	6122.5E-4	1.274.5E+15	1.274.5E+15
8.4	8.4	2.203E+06	2.0733E+06	2.0733E+06	248.47E+12	6122.5E-4	1.274.5E+15	1.274.5E+15
8.6	8.6	1.603E+06	1.2933E+06	1.2933E+06	254.67E+12	6122.5E-4	1.274.5E+15	1.274.5E+15
8.8	8.8	1.143E+06	5.1933E+05	5.1933E+05	260.87E+12	6122.5E-4	1.274.5E+15	1.274.5E+15
9.0	9.0	8.203E+05	3.6333E+05	3.6333E+05	267.07E+12	6122.5E-4	1.274.5E+15	1.274.5E+15
9.2	9.2	6.003E+05	2.0733E+05	2.0733E+05	273.27E+12	6122.5E-4	1.274.5E+15	1.274.5E+15
9.4	9.4	4.403E+05	1.2933E+05	1.2933E+05	279.47E+12	6122.5E-4	1.274.5E+15	1.274.5E+15
9.6	9.6	3.203E+05	5.1933E+04	5.1933E+04	285.67E+12	6122.5E-4	1.274.5E+15	1.274.5E+15
9.8	9.8	2.203E+05	3.6333E+04	3.6333E+04	291.87E+12	6122.5E-4	1.274.5E+15	1.274.5E+15
10.0	10.0	1.603E+05	2.0733E+04	2.0733E+04	298.07E+12	6122.5E-4	1.274.5E+15	1.274.5E+15
10.2	10.2	1.143E+05	1.2933E+04	1.2933E+04	304.27E+12	6122.5E-4	1.274.5E+15	1.274.5E+15
10.4	10.4	8.203E+04	5.1933E+03	5.1933E+03	310.47E+12	6122.5E-4	1.274.5E+15	1.274.5E+15
10.6	10.6	6.003E+04	3.6333E+03	3.6333E+03	316.67E+12	6122.5E-4	1.274.5E+15	1.274.5E+15
10.8	10.8	4.403E+04	2.0733E+03	2.0733E+03	322.87E+12	6122.5E-4	1.274.5E+15	1.274.5E+15
11.0	11.0	3.203E+04	1.2933E+03	1.2933E+03	329.07E+12	6122.5E-4	1.274.5E+15	1.274.5E+15
11.2	11.2	2.203E+04	5.1933E+02	5.1933E+02	335.27E+12	6122.5E-4	1.274.5E+15	1.274.5E+15
11.4	11.4	1.603E+04	3.6333E+02	3.6333E+02	341.47E+12	6122.5E-4	1.274.5E+15	1.274.5E+15
11.6	11.6	1.143E+04	2.0733E+02	2.0733E+02	347.67E+12	6122.5E-4	1.274.5E+15	1.274.5E+15
11.8	11.8	8.203E+03	1.2933E+02	1.2933E+02	353.87E+12	6122.5E-4	1.274.5E+15	1.274.5E+15
12.0	12.0	6.003E+03	5.1933E+01	5.1933E+01	360.07E+12	6122.5E-4	1.274.5E+15	1.274.5E+15
12.2	12.2	4.403E+03	3.6333E+01	3.6333E+01	366.27E+12	6122.5E-4	1.274.5E+15	1.274.5E+15
12.4	12.4	3.203E+03	2.0733E+01	2.0733E+01	372.47E+12	6122.5E-4	1.274.5E+15	1.274.5E+15
12.6	12.6	2.203E+03	1.2933E+01	1.2933E+01	378.67E+12	6122.5E-4	1.274.5E+15	1.274.5E+15
12.8	12.8	1.603E+03	5.1933E+00	5.1933E+00	384.87E+12	6122.5E-4	1.274.5E+15	1.274.5E+15
13.0	13.0	1.143E+03	3.6333E-01	3.6333E-01	391.07E+12	6122.5E-4	1.274.5E+15	1.274.5E+15
13.2	13.2	8.203E+02	2.0733E-01	2.0733E-01	397.27E+12	6122.5E-4	1.274.5E+15	1.274.5E+15
13.4	13.4	6.003E+02	1.2933E-01	1.2933E-01	403.47E+12	6122.5E-4	1.274.5E+15	1.274.5E+15
13.6	13.6	4.403E+02	5.1933E-01	5.1933E-01	409.67E+12	6122.5E-4	1.274.5E+15	1.274.5E+15
13.8	13.8	3.203E+02	3.6333E-01	3.6333E-01	415.87E+12	6122.5E-4	1.274.5E+15	1.274.5E+15
14.0	14.0	2.203E+02	2.0733E-01	2.0733E-01	422.07E+12	6122.5E-4	1.274.5E+15	1.274.5E+15
14.2	14.2	1.603E+02	1.2933E-01	1.2933E-01	428.27E+12	6122.5E-4	1.274.5E+15	1.274.5E+15
14.4	14.4	1.143E+02	5.1933E-01	5.1933E-01	434.47E+12	6122.5E-4	1.274.5E+15	1.274.5E+15
14.6	14.6	8.203E+01	3.6333E-01	3.6333E-01	440.67E+12	6122.5E-4	1.274.5E+15	1.274.5E+15
14.8	14.8	6.003E+01	2.0733E-01	2.0733E-01	446.87E+12	6122.5E-4	1.274.5E+15	1.274.5E+15
15.0	15.0	4.403E+01	1.2933E-01	1.2933E-01	453.07E+12	6122.5E-4	1.274.5E+15	1.274.5E+15
15.2	15.2	3.203E+01	5.1933E-01	5.1933E-01	459.27E+12	6122.5E-4	1.274.5E+15	1.274.5E+15
15.4	15.4	2.203E+01	3.6333E-01	3.6333E-01	465.47E+12	6122.5E-4	1.274.5E+15	1.274.5E+15
15.6	15.6	1.603E+01	2.0733E-01	2.0733E-01	471.67E+12	6122.5E-4	1.274.5E+15	1.274.5E+15
15.8	15.8	1.143E+01	1.2933E-01	1.2933E-01	477.87E+12	6122.5E-4	1.274.5E+15	1.274.5E+15
16.0	16.0	8.203E+00	5.1933E-01	5.1933E-01	484.07E+12	6122.5E-4	1.274.5E+15	1.274.5E+15
16.2	16.2	6.003E+00	3.6333E-01	3.6333E-01	490.27E+12	6122.5E-4	1.274.5E+15	1.274.5E+15
16.4	16.4	4.403E+00	2.0733E-01	2.0733E-01	496.47E+12	6122.5E-4	1.274.5E+15	1.274.5E+15
16.6	16.6	3.203E+00	1.2933E-01	1.2933E-01	502.67E+12	6122.5E-4	1.274.5E+15	1.274.5E+15
16.8	16.8	2.203E+00	5.1933E-01	5.1933E-01	508.87E+12	6122.5E-4	1.274.5E+15	1.274.5E+15
17.0	17.0	1.603E+00	3.6333E-01	3.6333E-01	515.07E+12	6122.5E-4	1.274.5E+15	1.274.5E+15
17.2	17.2	1.143E+00	2.0733E-01	2.0733E-01	521.27E+12	6122.5E-4	1.274.5E+15	1.274.5E+15
17.4	17.4	8.203E-01	1.2933E-01	1.2933E-01	527.47E+12	6122.5E-4	1.274.5E+15	1.274.5E+15
17.6	17.6	6.003E-01	5.1933E-01	5.1933E-01	533.67E+12	6122.5E-4	1.274.5E+15	1.274.5E+15
17.8	17.8	4.403E-01	3.6333E-01	3.6333E-01	539.87E+12	6122.5E-4	1.274.5E+15	1.274.5E+15
18.0	18.0	3.203E-01	2.0733E-01	2.0733E-01	546.07E+12	6122.5E-4	1.274.5E+15	1.274.5E+15
18.2	18.2	2.203E-01	1.2933E-01	1.2933E-01	552.27E+12	6122.5E-4	1.274.5E+15	1.274.5E+15

## VI Conclusions and Recommendations

### Conclusion

The RADHOT program implements a radiation transport scheme coupled with a hydrodynamics scheme that is reported to be both fast and fairly accurate in calculating the environment around a nuclear weapon at early times. The RADHOT code is currently unable to evaluate the preceding statement due to a lack of good opacity data. The opacity data currently in RADHOT makes the air around the source region highly opaque, resulting in a code optimized for situations characterized primarily for streaming, attempting to calculate the behavior of a diffusive regime. Correction of the opacity data is essential to any evaluation of the accuracy of the RADHOT code. The equation of state used in RADHOT also needs further work, i.e. the "Nickel-Doan Equation of State for Air" fit needs to be extended to  $10^6$  K.

The original approach in this thesis was to attempt to couple the radiation transport scheme described by Zinn to an existing hydrodynamics code (HUFF). A great amount of effort and time was required to understand and debug the HUFF code. Further, the final code resulting from this "forced marriage" is inefficient, for example, in the RADHOT code there are arrays of cell volumes and mass, cell densities, and cell specific volumes because the different parts of the program require different forms of the same quantity. Computing redundant quantities partially accounts for the slow cycle

time in RADHOT. Using a look-up table for the Planck function, as well as for the opacity data would also accelerate the cycle time.

A better approach would have been to program Zinn's radiation hydrodynamics scheme directly, allow it to run until shortly after hydroseparation (the starting point of HUFF), and then provide output compatible with the input requirements of HUFF. By running the two programs in series, the radiation hydrodynamics could be turned off when it is no longer significant, and HUFF would have its initial conditions corrected for radiation.

#### Recommendations

1. Obtain valid opacity data for RADHOT. This is the single most important item that needs to be accomplished.
2. Improve the equation of state fit by smoothly extending the Nickel-Doan fit of gamma to the ideal limit of 5/3.
3. Modify RADHOT so that at the completion of a run, it will provide input data to HUFF.
4. Incorporate look-up tables for the Planck function and for opacity data into RADHOT.
5. Incorporate programming techniques into RADHOT that can increase the execution speed.

## Bibliography

1. Glasstone, Samuel, editor. The Effects of Nuclear Weapons (Third Edition). Washington: United States Atomic Energy Commission, 1977.
2. Richtmeyer, Robert D. and K. W. Morton. Difference Methods for Initial-Value Problems (Second Edition). New York: Interscience Publishers, 1967.
3. Bridgman, Charles J. The Physics of Nuclear Explosives, Chap 5. (class notes). Wright-Patterson AFB, Ohio: Air Force Institute of Technology, March 1980.
4. Peters, David J. HUFF, A One-Dimensional Hydrodynamics Code for Strong Shocks. Master's Thesis. Wright-Patterson AFB, Ohio: Air Force Institute of Technology, December 1978. (ADA 063481).
5. Doan, L. R. and G. H. Nickel. A Subroutine for the Equation of State of Air. RTD (WLR) TM-63-2. Kirtland AFB, New Mexico: Air Force Weapons Laboratory, May 1963.
6. Zinn, John. "A Finite Difference Scheme for Time-Dependent Spherical Radiation Hydrodynamics Problems," Journal of Computational Physics, Vol. 13, (569-590). New York: Academic Press, Inc., 1973.
7. Landshoff, R. K. M., editor. Thermal Radiation Phenomena, Vol. 5, "Radiation Hydrodynamics of High Temperature Air." DASA 1917-5. Lockheed Missile and Space Company, Palo Alto, California. November 1967.
8. Pomraning, G. C. The Equations of Radiation Hydrodynamics. New York: Pergamon Press, 1973.
9. Selby, Samuel M., editor. Standard Mathematical Tables (Nineteenth Edition). Cleveland, Ohio: Chemical Rubber Corporation, 1971.
10. Harlow, Francis H. and Antony A. Amsden. Fluid Dynamics. LA 4700. Los Alamos, New Mexico: Los Alamos Scientific Laboratory of the University of California, June 1971.
11. Zel'dovich, Ya. B. and Yu. P. Raizer. Physics of Shock Waves and High-Temperature Hydrodynamic Phenomena. New York: Academic Press, Inc., 1966.
12. Landshoff, R.K.M., editor. Thermal Radiation Phenomena, Vol. 2, "The Equilibrium Radiative Properties of Air-Theory." DASA 1971-2. Lockheed Missile and Space Company, Palo Alto, California. May 1967.

## Appendix A

### Derivations

$$\Delta s(\theta) = R_2 \cos\theta - (R_1^2 - R_2^2 \sin^2\theta)^{\frac{1}{2}} \quad (A-1)$$

$$\Delta s(\theta_{2s}) = ? \quad \theta_{2s} = \sin^{-1} \frac{R_s}{R_2} \quad \text{for } R_1 > R_s \quad (A-2)$$

$$\Delta s(\theta_{2s}) = R_2 \cos\theta_{2s} - (R_1^2 - R_s^2)^{\frac{1}{2}} \quad (A-3)$$

$$\Delta s(\theta_{2s})^2 = R_2^2(1 - \sin^2\theta_{2s}) - R_2 \cos\theta_{2s} (R_1^2 - R_s^2)^{\frac{1}{2}} + R_1^2 - R_s^2 \quad (A-4)$$

$$\Delta s(\theta_{2s})^2 = R_2^2 \left(1 - \frac{R_s^2}{R_2^2}\right) - R_2 \cos\theta_{2s} (R_1^2 - R_s^2)^{\frac{1}{2}} + (R_1^2 - R_s^2) \quad (A-5)$$

$$\Delta s(\theta_{2s})^2 = (R_2^2 - R_s^2) - R_2 \cos\theta_{2s} (R_1^2 - R_s^2)^{\frac{1}{2}} + (R_1^2 - R_s^2) \quad (A-6)$$

$$\Delta s(\theta_{2s})^2 = (R_2^2 - R_s^2) - (R_2^2 \cos^2\theta_{2s} (R_1^2 - R_s^2))^{\frac{1}{2}} + (R_1^2 - R_s^2) \quad (A-7)$$

$$\Delta s(\theta_{2s})^2 = (R_2^2 - R_s^2) - (R_2^2 (1 - \sin^2\theta_{2s}) (R_1^2 - R_s^2))^{\frac{1}{2}} + (R_1^2 - R_s^2) \quad (A-8)$$

$$\Delta s(\theta_{2s})^2 = (R_2^2 - R_s^2) - (R_2^2 - R_s^2) (R_1^2 - R_s^2)^{\frac{1}{2}} + (R_1^2 - R_s^2) \quad (A-9)$$

$$\therefore \Delta s(\theta_{2s}) = ((R_2^2 - R_s^2) - (R_1^2 - R_s^2))^{\frac{1}{2}} \quad (A-10)$$

$$u(\theta_{2s}) = \mu' \Delta s(\theta_{2s}) = \frac{\tau}{(R_2 - R_1)} \Delta s(\theta_{2s}) \quad (A-11)$$

$$u(\theta_{2S}) = (\tau/\Delta R) ((R_2^2 - R_S^2) - (R_1^2 - R_2^2))^{1/2} \quad (71)$$

$$u_m = u(\theta_m) \quad \theta_m = \sin^{-1} \frac{R_1}{R_2} \quad (A-12)$$

$$u(\theta) = \mu' \Delta s(\theta) = \mu' (R_2 \cos \theta - (R_1^2 - R_2^2 \sin^2 \theta)^{1/2}) \quad (A-13)$$

$$\Delta s(\theta_m) = R_2 \cos \theta_m - (R_1^2 - R_2^2 \sin^2 \theta_m)^{1/2} \quad (A-14)$$

$$\Delta s(\theta_m) = R_2 \cos \theta_m - (R_1^2 - R_2^2 \frac{R_1^2}{R_2^2})^{1/2} \quad (A-15)$$

$$\Delta s(\theta_m) = R_2 \cos \theta_m - (R_1^2 - R_1^2) \quad (A-16)$$

$$\Delta s(\theta_m) = R_2 \cos \theta_m \quad (A-17)$$

$$\Delta s(\theta_m)^2 = R_2^2 \cos^2 \theta_m = R_2^2 (1 - \sin^2 \theta_m) \quad (A-18)$$

$$\Delta s(\theta_m)^2 = R_2^2 (1 - \frac{R_1^2}{R_2^2}) \quad (A-19)$$

$$\Delta s(\theta_m)^2 = R_2^2 - R_1^2 \quad (A-20)$$

$$\Delta s(\theta_m) = ((R_2 + R_1)(R_2 - R_1))^{1/2} \quad (A-21)$$

$$u(\theta_m) = \mu' \Delta s(\theta_m) = (\tau / (R_2 - R_1)) ((R_2 + R_1)(R_2 - R_1))^{1/2} \quad (A-22)$$

$$u(\theta_m) = \tau ((R_2 + R_1) / (R_2 - R_1))^{1/2} \quad (72)$$

## Appendix B

### User's Guide for RADHOT

This appendix describes the data card input and the NOS/BE control cards, and selecting the output when operating program RADHOT. The data card input will be presented first followed by a discussion of the NOS/BE control cards required to run RADHOT.

#### Data Cards for RADHOT

RADHOT is designed to solve the problem of a nuclear detonation in air. Due to the initial mesh spacing being fixed in the program (subroutine BLAST), the program as it currently exists can only solve this problem for 1MT of yield at sea level. Addition of a scaling parameter for the initial mesh spacing will allow the program to be run for different yields and altitudes. This users guide will define what data is required, and what the value of the data is currently fixed at.

#### Parameters

##### 1. Card 1-FLAG(2), FLAG(3), FLAG(4), TSTOP

This card contains the input flags defined as follows:

FLAG(2) is an integer representing the number of result times listed on card 2.

FLAG(3) is an integer representing the maximum number of timestep iterations. The program will stop if it reaches this many iterations.

FLAGS(4) is an integer representing the type of problem

to be solved. FLAG(4) must be 3.

TSTOP is the maximum problem time allowed. The program will stop if it reaches this time. Results for this time will be plotted in addition to those on card 2.

2. Card 2-TABLE(1), TABLE(2),..., TABLE(FLAG(2)). This card lists the requested result times. A maximum of 10 times can be listed due to the dimension of the array TABLE.
3. Card 4-MAXNU. Number of frequency groups used in the problem. Maximum value is 8, though because of the current poor opacity data in subroutine AMU, there is no advantage to having more than one group.

#### Problem Defining Card

Card 3-YKT, SP, DS, ST is the problem defining card.

The variables are: YKT-Yield of the blast in kilotons.  
currently fixed at 1000 (1MT)

SP, DS, ST-altitude scaling factors from Table 1 of the  
text. Currently fixed for sea level.

#### Current Data Set

The following data cards are being run with RADHOT:

```
5 10000 3 1.  
1.E-6 5.E-5 3.E-4 9.E-2 .8  
1000. 1. 1. 1.  
1
```

#### NOS/BE Control Cards for RADHOT

This section presents the control cards necessary to

execute the RADHOT program at AFIT.

Permanent File. To place RADHOT on permanent file, the following cards are necessary:

```
job. problem
REQUEST, RADHOT, *PF.
COPYBR, INPUT, RADHOT.
CATALOG, RADHOT, RP=999.
7/8/9
RADHOT deck.
7/8/9
6/7/8/9
```

after RADHOT is on permanent file, the following control cards are used to run the program.

```
job, T200, CM75000. problem
ATTACH,IMSL, ID=LIBRARY, SN=ASD.
LIBRARY,IMSL
ATTACH,RADHOT.
FTN,I=RADHOT,OPT=2.
LGO.
7/8/9
DATA cards for RADHOT
7/8/9
6/7/8/9.
```

## Appendix C

### RADHOT Program Listing

```
100      SUBROUTINE RADHOT(INPUT,400,OUTPUT,TAPE1,TINPUT,TAPE2,OUTPUT
110      I,FILEG,REVIEW,TABLE7,FILES,TAPES,REVIEW)
120      DIMENSION FLAG(5),TABLE(10)
130      INTEGER FLAG
140      CALL FLAGS(FLAG, TABLE, TSTOP)
150      CALL CONTROL(FLAG, TABLE, TSTOP)
160      PRINT*, "TIME LIMIT EXCEEDED"
170      STOP
180      END
190=C
200      SUBROUTINE FLAGS(FLAG, TABLE, TSTOP)
210      DIMENSION FLAG(5),TABLE(10)
220      INTEGER FLAG
230=C----- INITIALIZE CONTROL PARAMETERS -----
240      DO 10 I=1,3
250      10 FLAG(I)=0
260      FLAG(5) = 1
270      DO 30 I=1,10
280      30 TABLE(I)=0
290=C      I READ FLAGS AND REAL TIME LIMIT           I
300=C      I     FLAG(2)=# OF TABLES REQUESTED        I
310=C      I     FLAG(3)=# OF CYCLES THROUGH HYDRO       I
320=C      I     FLAG(5)=1# INDICATES FIRST PROGRAM ITERATION
330      READ*,(FLAG(I),I=2,4),TSTOP
340=C----- READ REQUESTED TABLE TIMES -----
350      IF2=FLAG(2)
360      READ*,(TABLE(I),I=1,IF2)
370=C-----WRITE OUT INFORMATION PROVIDED BY FLAGS -----
380      WRITE(2,400)
390      WRITE(2,700)
400      WRITE(2,200)FLAG(2),(TABLE(I),I=1,IF2)
410      WRITE(2,300)TSTOP,FLAG(3)
420      200 FORMAT(////,T10,"TABLES FOR THE FOLLOWING ",I3,
430      1" TIMES WERE REQUESTED:",//,2(T15,5(1PE10.3,2X),/))
440      300 FORMAT(////,T10,"MAX TIME TO RUN IS ",F4.1," SEC."
450      1,/,T10,"NoX CYCLES THROUGH Timestep IS ",I9,".")
460      400 FORMAT(1H1,T40,"THIS IS A BLAST PROBLEM")
470      600 FORMAT(1H1,T40,"NO SUCH PROBLEM NUMBER = ",I3)
480      700 FORMAT(T24,"RADIATION EFFECTS HAVE BEEN INCORPORATED AT EARLY T
490      1S")
500      RETURN
510      END
520
530      SUBROUTINE CONTROL(FLAG, TABLE, TSTOP)
540      DIMENSION X(101),U(101),P(101),D(101),Q(101),FLAG(5)
550      1, TABLE(10),CK(7),BEDT(101),EI(101),TEMP(101),ER(101)
```



```

1100= DO 10 II=1,N
1110=C-- CALL TO ADVANCE ONE TIME STEP -----
1120=      CALL HYDRO(D,P,X,Q,VEL,DX,CA,L,RHO,GAMMA,N1,DT,TIME,FLAG,C2,
1130=      MAXNU,EI,DELT,WTTEMP,TEMP,ER,F,AMASS,VN,VO,V,DELV,VG)
1140=      DO 10 I =1,100
1150=      DEIT(I)=BLURCUM(VG(I)-VG(I))
1160=      EI(I)=EI(I)+DEIT(I)
1170=      IF(EI(I).LT.0) EI(I)=3.308E6
1180=      TEMP(I)=TEMPER(EI(I),TEMP(I),VN(I))
1190=      VG(I)=5./3.
1200=      XXX=RHO
1210=      IF(I.EQ.1) XXX=0.3386
1220=      TST=0.8*(EI(1)/EI(I))
1230=      IF(TST.LT.0.01) VG(I)=VGAMMA(EI(I),D(I),XXX)
1240=      10 P(I)=(VG(I)-1)*EI(I)*D(I)
1250=C-----CALL TO SET BOUNDARY CONDITIONS AND TRACK SHOCK -----
1260=      CALL EXPAND(CA,LALPHA,N1,DX,RHO,P,D,X,Q,U,DT,CK,FLAG(5))
1270=      TIME=CR(2)
1280=      FLAG(5)=0
1290=C----- CALL TO COPY REQUESTED TABLES -----
1300=      IF(TIME.GE.TSTOP.CR.TIME.GE.TABLE(1))
1310=      1CALL COPY(X,U,P,D,Q,FLAG(2),TIME,TABLE,CK,TEMP)
1320=C----- ABORT IF TIME LIMIT REACHED -----
1330=      IF(TIME.GE.TSTOP)RETURN
1340=C----- CALL FOR REZONE IF REQUIRED -----
1350=      IF(N1.LT.94) GO TO 15
1360=      CALL REZONE(X,U,P,D,Q,DX,GAMMA,ICYCLE,TIME,N1,RHO)
1370=      PRINT*, "AFTER REZONE"
1380=      CALL WRITER(TEMP,P,D,EI,X,DELT,ER,F)
1390=      15 CONTINUE
1400=C----- CALL RESULTS AND ABORT PROGRAM IF CYCLE LIMIT REACHED -----
1410=      CALL COPY(X,U,P,D,Q,FLAG(2),TIME,TABLE,CK,TEMP)
1420=      PRINT*, "YOU REACHED THE CYCLE LIMIT OF ",ICYCLE
1430=      PRINT*, "TIME IS ",TIME," SEC."
1440=      RETURN
1450=      END
1460=C
1470=      SUBROUTINE HYDRO(D,P,X,Q,VEL,DX,CA,L,RHO,GAMMA,N1,DT,TIME,FLAG,C2,
1480=      MAXNU,EI,DELT,WTTEMP,TEMP,ER,F,AMASS,VN,VO,V,DELV,VG)
1490=      DIMENSION D(10),P(101),X(101),Q(101),U(101),FLAG(5)
1500=      1,VG(101),VEL(101),AVGNU(101),EI(101),DELT(101),VO(101),VN(1
1510=      101),TEMP(101),NSFLTR(10),D(101,10),DEITR(101),ER(101)
1520=      DIMENSION F(2,101,10),AMASS(101),DELR(101)
1530=      DIMENSION V(101),DELV(101)
1540=C---- R=G/CM**3, P=D/CM**2, TEMP=KELVIN, EI=ER=ERGS/CM**3, VO=VN=CM**3/G
1550=      INTEGER FLAG
1560=C----- INITIALIZE LOCAL PARAMETERS -----
1570=      VEL(1)=0
1580=      PI=ACOS(-1.)
1590=      QMAX=.01
1600=      DO 40 I=1,100
1610=      C=SRRT(VG(I)*P(I)/D(I))
1620=C----- COMPUTE NEW VISCOSITIES -----
1630=      Q(I)=0.5*P(I)*DELV(I)/(D(I)*(X(I)**24*(I+1)**2)*C)
1640=      IF((VEL(I+1)-VEL(I)).GE.0.) Q(I)=0.
1650=      40 CONTINUE

```

```

1650= 40 CONTINUE
1660=     DELR(I)=0,
1670=     DO 42 I=1,99
1680=       VEL(I)=P(I)*X(I)+Q(I)*(1.0+DT)/(AMASS(I)+AMASS(I+1))
1690=     VEL(1)=VEL(1)+ACC*DT
1700=     42 DELR(I+1) = DT*(VEL(I+1)+0.5*ACC*DT)
1710=     DO 45 I = 1,99
1720=C----- ASSUMES AIR BEHAVES AS AN IDEAL GAS DURING RADIATION PHASE
1730=     ET(I)=ET(I)+4.*PI*(P(I)+Q(I))*(X(I)**2*AMASS(I)-X(I+1)**2*AMASS(I+1))
1740=     1/AMASS(I)
1750=     X(I+1)=X(I+1) + DELR(I+1)
1760=     45 CONTINUE
1770=C----- LOCATE NEW SHOCK POSITION -----
1780=     DO 50 I=1,100
1790=       VO(I)=1./D(I)
1800=       VOL0=V(I)
1810=       V(I)=4./3.*PI*(X(I+1)**3-X(I)**3)
1820=       D(I)=AMASS(I)/V(I)
1830=       DELV(I)=ABS(V(I)-VOL0)
1840=       VN(I)=1./D(I)
1850=     50 CONTINUE
1860=     DO 52 I=1,100
1870=       IF(QMAX.GT.Q(I))GO TO 52
1880=       QMAX=Q(I)
1890=       N1=I+1
1900=     52 CONTINUE
1910=     RETURN
1920=   END
1930=   SUBROUTINE BLAST(CA,L,N1,DX,RHO,F,D,X,Q,U,DT,CK,V,DELV)
1940=   DIMENSION P(101),D(101),X(101),Q(101),U(101),CK(7),V(101),DELV(101)
1950=   1)
1960=   CA=4
1970=   PI=ACOS(-1.)
1980=C----- READ YIELD SCALING PARAMETERS, AND PROBLEM GEOMETRY -----
1990=   READ*,YKT,SP,SD,ST
2000=   L=3
2010=   WRITE*,YKT,SP,SD,ST,L
2020=C----- COMPUTE INITIAL CONDITIONS USING SCALING LAWS -----
2030=   PNORM=1.014E6*SP
2040=   CK(2)=TIME=1.E-7
2050=   PBLAST=9.8E13
2060=   DX=89.
2070=   CK(1) = YKT
2080=   RHO=1.293E-3*SD
2090=   N1=1
2100=   CK(5)=PNORM
2110=   PRINT*, "PNORM=",PNORM," PBLAST=",PBLAST
2120=   PRINT*, " TIME=",TIME," DX=",DX," RHO=",RHO," N1=",N1
2130=C----- ASSIGN SCALED VALUES TO PROBLEM ARRAYS -----
2140=   DO 10 I=1,101
2150=     Q(I)=U(I)=0
2160=     D(I)=RHO
2170=     IF(I.EQ.1)X(I)=0
2180=     IF(I.GT.1)X(I)=X(I-1)+DX
2190=     IF(I.LE.N1)P(I)=PBLAST
2200=     IF(I.GT.N1)P(I)=PNORM

```

```

2200=      IF(T.GT.N1)P(I)=PNORM
2210=      DO 10 U(I,T)= 0.
2220=      DO 20 I= 1,100
2230=      U(I)=4./3.*P(I)*(X(I+1)**3-X(I)**3)
2240=      20 CONTINUE
2250=      CK(3)= OPOS = X(2)
2260=      RETURN
2270=      END
2280=C
2290=      SUBROUTINE EXPAND(CA,L,N1,DX,RHO,P,D,X,Q,U,DT,CK,FLAG)
2300=      DIMENSION P(101),D(101),X(101),Q(101),U(101),CK(7)
2310=      INTEGER FLAG
2320=      IF(FLAG.EQ.1) TIMIT=KFIFTY=CYCLE=0
2330=C----- RESET SYMETRIC P. C. AND ADVANCE TIME -----
2340=      X(1)=U(1)=0.
2350=      IF(FLAG.EQ.1) PNORM=CK(5)
2360=      IF(FLAG.EQ.1) TIME=CK(2)
2370=C----- LOCATE NEW SHOCK POSITION -----
2380=      IP=N1
2390=C----- TIME SHOCK PROGRESS FOR 50 ITERATIONS -----
2400=      KFIFTY=KFIFTY+1
2410=      TIMIT=TIMIT+DT
2420=C----- COMPUTE OVERPRESSURE AND OVERDENSITY -----
2430=      PMAX=IMAX=UMAX=0.
2440=      DO 20 I=1,100
2450=      IF(U(I).GT.UMAX)UMAX=U(I)
2460=      IF(P(I).GT.PMAX)PMAX=P(I)
2470=      IF(D(I).GT.IMAX)IMAX=D(I)
2480=      20 CONTINUE
2490=      CK(5)=OP=PMAX-PNORM
2500=      CK(6)=OD=IMAX-RHO
2510=C----- PLACE COMPUTED VALUES IN CHECK (CK) ARRAY -----
2520=      CK(1)=CYCLE=CYCLE+1.
2530=      CK(2)=TIME=TIME+DT
2540=      CK(3)=DT
2550=      CK(4)=POS=X(IP)
2560=C----- COMPUTE NEW SHOCK MATERIAL VELOCITY -----
2570=      CK(7)=UMAX
2580=      IF(KFIFTY.LT.50) GO TO 30
2590=      OPOS=POS
2600=      TIMIT=KFIFTY=0
2610=C----- WRITE CHECK VALUES EVERY 50 ITERATIONS -----
2620=      WRITE(8,2000)(CK(I),I=1,7)
2630=      WRITE(2,100)(CK(K),K=1,7)
2640=      100 FORMAT(2X,"CYCLE=",F6.0," TIME=",1PE9.3," DT=",E9.3,
2650=      1," S POS =",E9.3," 0 PRES=",E9.3," 0 DENS=E9.3," S VEL=",
2660=      2,E9.3)
2670=      2000 FORMAT(1X,"CYCLE=",F5.0," T(SEC)=",1PE9.2," DT(SEC)="
2680=      1,E7.0," POS(CM)=",E9.2," OP(D/CM**2)=",E9.2," OI(G/CM**3)="
2690=      2,E9.2," DVEL(CM/SEC)=",E9.2)
2700=      30 RETURN
2710=      END
2720=C
2730=      SUBROUTINE REZON(X,U,P,D,Q,DX,GAMMA,TCYCLE,TIME,N1,RHO)
2740=      DIMENSION X(101),U(101),P(101),D(101),Q(101)
2750=      N1=N1/2

```

```

2750=      N1=N1/2
2760=      WRITE(2,100)TML, CYCLE
2770=      DO 10 J=1,97,2
2780=      T=(J+1)/2
2790=C      COMPUTE GAMMAS -----
2800=      EIJJ1=EIJA(P(J),D(J),RHO)
2810=      EIJJ2=EIJA(P(J+1),D(J+1),RHO)
2820=      AGAMA=VGAMMA(EIJJ1,D(J),RHO)
2830=      BGAMA=VGAMMA(EIJJ2,D(J+1),RHO)
2840=C      COMPUTE MASS AND NEW DENSITY -----
2850=      XMJ1=D(J)*(X(J+1)**3-X(J)**3)
2860=      XMJ2=D(J+1)*(X(J+2)**3-X(J+1)**3)
2870=      PUD(I,3)=(XMJ1+XMJ2)/(X(J+2)**3-X(J)**3)
2880=      XMI1=PUD(I,3)*(X(J+2)**3-X(J)**3)
2890=C      COMPUTE OLD CELL CENTERED VELOCITY -----
2900=      UJ1=(U(J)+U(J+1))/2,
2910=      UJ2=(U(J+1)+U(J+2))/2,
2920=C      COMPUTE OLD ENERGIES (KINETIC, INTERNAL, TOTAL) ---
2930=      EKJ1=UJ1**2/2,
2940=      EKJ2=UJ2**2/2,
2950=      EIJJ1=P(J)/((AGAMA-1.)*D(J))
2960=      EIJJ2=P(J+1)/((BGAMA-1.)*D(J+1))
2970=      ETJJ1=EKJ1+EIJJ1
2980=      ETJJ2=EKJ2+EIJJ2
2990=C      COMPUTE NEW TOTAL ENERGY -----
3000=      ETII=(XMJ1*ETJJ1+XMJ2*ETJJ2)/XMI1
3010=C      COMPUTE MOMENTUM -----
3020=      XMOMJ1=XMJ1*UJ1
3030=      XMOMJ2=XMJ2*UJ2
3040=      PUD(I,2)=(XMOMJ1+XMOMJ2)/XMI1
3050=      XMOMI1=XMI1*PUD(I,2)
3060=C      COMPUTE NEW KINETIC AND INTERNAL ENERGY -----
3070=      EKII=PUD(I,2)**2/2,
3080=      EIII=ETII-EKII
3090=C      COMPUTE NEW PRESSURE -----
3100=      GAMMA=VGAMMA(EIII,PUD(I,3),RHO)
3110=      PUD(I,1)=EIII*(GAMMA-1.)*PUD(I,3)
3120=C      BYPASS LENGTHY REZONE PRINTOUT -----
3130=      IF(N1.GT.10)GO TO 10
3140=      WRITE(2,200)X(J),UJ1,P(J),D(J),XMJ1,XMOMJ1,ETJJ1,EKJJ1,EIJJ1
3150=      WRITE(2,200)X(J+1),UJ2,P(J+1),D(J+1),XMJ2,XMOMJ2,ETJJ2,EKJJ2,EIJJ2
3160=      WRITE(2,250)X(J),UJ1,PUD(I,1),PUD(I,3),XMI1,XMOMI1,ETII,EKII,EIII
3170=      10 CONTINUE
3180=C      ASSIGN VELOCITY FOR CENTER AND RESET DX -----
3190=      PUD(I,2)=0
3200=      DX=2.*DX
3210=C      STORE NEW VALUES IN PROGRAM ARRAYS -----
3220=      DO 20 I=1,49
3230=      J=2*I-1
3240=      X(I)=X(J)
3250=      P(I)=PUD(I,1)
3260=      D(I)=PUD(I,3)
3270=      IF(I.EQ.1)GO TO 20
3280=C      COMPUTE NEW BOUNDARY VELOCITIES -----
3290=      U(I)=(PUD(I-1,2)+PUD(I,2))/2,
3300=      20 CONTINUE

```

```

3300= 20 CONTINUE
3310=C----- DEFINE VALUES FOR UPPER HALF OF ARRAYS -----
3320= DO 25 I=50,101
3330= X(I)=X(I-1)+DX
3340= U(I)=Q(I)=0
3350= P(I)=P(101)
3360= D(I)=D(101)
3370= 25 CONTINUE
3380=C----- COMPUTE NEW VISCOSITY -----
3390= DO 30 I=1,50
3400= Q(I)=3.*B(I)*(U(I+1)-U(I))**2
3410= IF(U(I+1)-U(I).GE.0)Q(I)=0
3420= 30 CONTINUE
3430=C----- SET BOUNDARY CONDITIONS -----
3440= U(1)=X(1)=0
3450= P(1)=P(2)
3460= Q(1)=Q(2)
3470= D(1)=D(2)
3480= 100 FORMAT(1H1,T20,"REZONE TIME = ",G9.3," ITERATION NUMBER ",I7,
3490= 1////,T4,"POSITION",T18,"VELOCITY",T32,"PRESSURE",T46,"DENSITY",
3500= T162,"MASS",T74,"MOMENTUM",T89,"T ENERGY",T102,"K ENERGY",
3510= T116,"I ENERGY",/,T7,"CM",T19,"CM/SEC",T33,"D/CM**3",
3520= 4T46,"G/CM**3",T63,"GM",T76,"G-SEC",T91,"ERG/G",T105,"ERG/G",
3530= 5T119,"ERG/G",///)
3540= 200 FORMAT(3X,9(G9.3,5X))
3550= 250 FORMAT(5X,9(G9.3,5X),/)
3560= RETURN
3570= END
3580=
3590= FUNCTION VOAMMA(EI,D,RHO)
3600=C----- HUFF ROUGH VARIABLE GAMMA COMPUTATION -----
3610= E1E=EI/1.E10
3620= IF(E1E.GT..1315)GO TO 10
3630= GMONE=.3981
3640= GO TO 30
3650= 10 CONTINUE
3660= IF(E1E.GT.1.)GO TO 20
3670= GMONE=-.0399*(E1E-.1315)**2+.3981
3680= GO TO 30
3690= 20 CONTINUE
3700= GMONE=.16+.624/(2.+E1E)
3710=C----- ADJUSTMENT FOR DENSITY -----
3720= RHOZ=D/RHO
3730= EL=ALOG10(E1E)
3740= ALPHA=.0577*EL-.0219*EL**2+.0035*EL**3+.00021*EL**4
3750= GMONE=GMONE*ALPHAZ*ALPHA
3760= 30 VOAMMA=GMONE*1.
3770= RETURN
3780= END
3790=
3800= SUBROUTINE COPY(X,U,P,D,Q,FLAG,TIME,TABLE,CODE)
3810= DIMENSION XC(10),UC(10),PC(10),DC(10),QC(10),AT(10),
3820= 1,CK(2),IT(10)
3830= INTEGER FLAG
3840=C----- RESET CALLING PARAMETERS -----
3850= FLAG=FLAG-1

```

```

3810=      FLAG=FLAG+1
3820=      DO 10 I=1,9
3830=      10 TABLE(I)=TABLE(I)
3840=      IF(FLAG.LT.0)TABLE(1)=1000.
3850=C----- WRITE INFORMATION ON LOCAL FILE (FILES) -----
3860=      ENTRY TCOPY
3870=      WRTIV(Z,1000)TIME,(X(I),U(I),P(I),D(I),Q(I),I=1,101)
3880=      WRITE(Z,2000)(CK(K),K=1,7)
3890=      WRITE(Z,1010)TIME
3900=      CALL PLOTSM(X,P,100)
3910=      WRITE(Z,2000)(CK(K),K=1,7)
3920=      WRITE(Z,1040)TIME
3930=      CALL PLOTSM(X,TEMP,100)
3940=      WRITE(Z,2000)(CK(K),K=1,7)
3950=      WRITE(Z,1020)TIME
3960=      CALL PLOTSM(X,D,100)
3970=      WRITE(Z,2000)(CK(K),K=1,7)
3980=      WRITE(Z,1001)TIME
3990=      CALL PLOTSM(X,U,100)
4000=      WRITE(Z,2000)(CK(K),K=1,7)
4010=      WRITE(Z,1030)TIME
4020=      CALL PLOTSM(X,Q,100)
4030=      WRITE(Z,2000)(CK(K),K=1,7)
4040=      WRITE(Z,1050)TIME
4050=      CALL PLOTSM(X,R,100)
4060=      WRITE(Z,2000)(CK(K),K=1,7)
4070=      WRITE(Z,2000)(CK(K),K=1,7)
4080= 1000 FORMAT(1X,"TIME IS",F9.5,"SEC",//,T7,"POSITION",T22
4090=   1,"VELOCITY",T37,"PRESSURE",T52,"DENSITY",T62,"VISCOSITY"
4100=   2,/,T9,"(CM)",T22,"(CM/SEC)",T37,"(D/CM**2)",T51,"(G/CM**3)"
4110=   3,T62,"(D/CM**2)",//,101(5(5X,1PE10,3),/))
4120= 1001 FORMAT(1H1,T40,"VELOCITY(CM/SEC) VS POSITION(CM) AT TIME = "
4130=   1,1PE10,3," SEC")
4140= 1010 FORMAT(1H1,T40,"PRESSURE(D/CM**2) VS POSITION(CM) AT TIME = "
4150=   1,1PE10,3," SEC")
4160= 1020 FORMAT(1H1,T40,"DENSITY(G/CM**3) VS POSITION(CM) AT TIME = "
4170=   1,1PE10,3," SEC")
4180= 1030 FORMAT(1H1,T40,"VISCOSITY(D/CM**2) VS POSITION(CM) AT TIME = "
4190=   1,1PE10,3," SEC")
4200= 1040 FORMAT(1H1,T40,"TEMPERATURE(KELVIN) VS POSITION(CM) AT TIME = "
4210=   1,1PE10,3," SEC")
4220= 2000 FORMAT(1X,"CYCLE=",F5.0," T(SEC)=",1PE9.2," DT(SEC)="
4230=   1,E7.0," POS(CM)=",E9.2," DP(D/CM**2)=",E9.2," DD(G/CM**3)="
4240=   2,E9.2," MVEL(CM/SEC)=",E9.2)
4250=      RETURN
4260=      END
4270=
4280=      SUBROUTINE PLOTSM(X,Y,N)
4290=      DIMENSION X(100),Y(100),W(100,40),WL(40)
4300=      NPI=N+1
4310=      DATA SLASH,HOT,STAR,OH,BLANK/1H/,1H,*,1H*,1H0,* */
4320=      XMAX=X(N+1)
4330=      YMAX=YMIN=0
4340=      DO 10 I=1,N
4350=      IF(Y(I).GT.YMAX)YMAX=Y(I)
4360=      IF(Y(I).LT.YMIN)YMIN=Y(I)
4370=      10 CONTINUE
4380=      YOVER=YMAX-Y(100)
4390=      DO 20 J=1,100
4400=      DO 20 J=1,40

```

AD-A100 637

AIR FORCE INST OF TECH WRIGHT-PATTERSON AFB OH SCHOOL--ETC F/G 12/1  
RADHOT: A RADIATION HYDRODYNAMICS CODE FOR WEAPON EFFECTS CALCULUS--ETC(U)  
MAR 81 D P WADE

UNCLASSIFIED AFIT/GNE/PH/81-10

2 rev 2  
AF  
DRAFT



NL

END  
DATE FILMED  
7-81  
DTIC

```

4400= DO 20 J=1,40
4410= W(I,J)=BLANK
4420= IF(I,ER,1)W(I,J)=SLASH
4430= C,I,O,10)I<J) PBT
4440= W(10,20)=W(20,20)=W(30,20)=W(40,20)=W(50,20)=W(99,20)="0"
4450= W(60,20)=W(70,20)=W(80,20)=W(90,20)=W(100,20)="0"
4460= W(9,20)=W(98,20)="1"
4470= W(19,20)="2"
4480= W(29,20)="3"
4490= W(39,20)="4"
4500= W(49,20)="5"
4510= W(59,20)="6"
4520= W(69,20)="7"
4530= W(79,20)="8"
4540= W(89,20)="9"
4550= 20 CONTINUE
4560= SCALE=YMAX/20.
4570= STORE=-YMIN/20.
4580= IF(SCALE.LT.STORE)SCALE=STORE
4590= DX=XMAX/5.
4600= SCALE=SCALE+.1*SCALE
4610= GMAX=20.*SCALE
4620= DO 30 I=1,21
4630= XIM1=(I-1)
4640= STORE=XIM1*SCALE
4650= K=21-I
4660= L=19+I
4670= WL(L)=-STORE
4680= WL(K)=STORE
4690= 30 CONTINUE
4700= DO 40 I=1,26,5
4710= J=4*(I-1)
4720= XI=(I-1)/5
4730= WL(I)=XI*DX
4740= 40 CONTINUE
4750= DXX=XMAX/100.
4760= DO 50 I=1,N
4770= DO 44 K=1,N
4780= XK=K
4790= IF(X(I).GT.XK*DXX-DXX/2.,AND.X(I).LE.XK*DXX+DXX/2.)GO TO 45
4800= 44 CONTINUE
4810= 45 CONTINUE
4820= DO 50 J=1,40
4830= XJM1=J-1
4840= XJ=J
4850= IF((GMAX-XJM1*SCALE.GT.Y(I)).AND.(GMAX-XJ*SCALE
4860= 1.LE.Y(I)))W(K,J)=OH
4870= 50 CONTINUE
4880= WRITE(2,100)XMAX,YMAX,YMIN,YOVER
4890= K=5
4900= WRITE(2,200)GMAX
4910= DO 60 J=1,40
4920= IF(J,ER,K)GO TO 55
4930= WRITE(2,400)(W(I,J),I=1,N)
4940= GO TO 60
4950= 55 K=K+5

```

```

4950= 55 K=R+5
4960=      WRITE(2,200)WL(J),W(I,J),T=J,N)
4970=      200 FORMAT(1X,200)(WL(I),I=1,23,5)
4980=      100 FORMAT(//,,T30,"THIS PLOT HAS XMAX= ",1PE10.3,,YMAX= "
5000=           1E10.3,,YMIN= ",E10.3," AND Y OVER= ",E10.3,///)
5010=      200 FORMAT(5X,E10.3,2X,100A1)
5020=      300 FORMAT(//,,T14,6(1PE10.3,10X))
5030=      400 FORMAT(17X,100A1)
5040=      RETURN
5050=      END
5060=C
5070=      SUBROUTINE RADFLO(MAXNU,R,DT,DEDT,TEMP,RSFEAR,B,ER,F,D,AVGNU,RHO)
5080=      DIMENSION R(101),RSFEAR(10),F(2,101,10),DEDT(101)
5090=      DIMENSION D(101),AVGNU(10)
5100=      DIMENSION B(101,10),TEMP(101),ER(101)
5110=C----- R=CM, TEMP=KELVIN, ER=ERGS/CM**3, DEDT=ERGS/(CM**3-SEC)-----
5120=C----- F=B=ERGS/(CM**2-SEC), RSFEAR=1/CM -----
5130=      PI=ACOS(-1.)
5140=      DO 30 NU = 1,MAXNU
5150=      F(1,101,NU) = 0.
5160=      F(1,1,NU) = 0.
5170=      F(2,1,NU) = 0.
5180=      DO 15 J = 1,99
5190=      I = 101 - J
5200=      PIR=PI*B(I,NU)
5210=      XXX=RHO
5220=      RM1= R(I+1) - R(I)
5230=      TAU=RM1*AMU(D(I),TEMP(I),AVGNU(NU),RHO)
5240=      UMAX= TAU * SQRT((R(I+1)+R(I)) / RM1)
5250=      IF(I.EQ.2) XXX=0.3386
5260=      TAUM=(R(I)-R(I-1))*AMU(D(I-1),TEMP(I-1),1.,XXX)
5270=C      IF(TAU.GT.2..AND.TAUM.GT.2.) GO TO 5
5280=      GO TO 10
5290=      5 F(1,I,NU) =ABS(8.*PI * (B(I-1,NU) - B(I,NU)) /(3.*(TAU + TAUM)))
5300=      GO TO 15
5310=      10 F(1,I,NU) = PIR +(F(1,I+1,NU)- PIR) * (((R(I+1)+R(I)) *TAU
5320=           1)**2 / (4. * R(I)**2) * (G(TAU) - G(UMAX)) - RM1**2 / (2.*
5330=           2(R(I) * TAU)**2) * (H(TAU) - H(UMAX)))
5340=      15 CONTINUE
5350=      DO 30 I = 1,100
5360=      XXX=RHO
5370=      RS2 = RSFEAR(NU) ** 2
5380=      RM1 = R(I+1) - R(I)
5390=      IF(I.EQ.1) XXX=0.3386
5400=      TAU=RM1*AMU(D(I),TEMP(I),AVGNU(NU),XXX)
5410=      IF(I.NE.100) TAUP=(R(I+2)-R(I+1))*AMU(D(I+1),TEMP(I+1),1.,RHO)
5420=C      IF(TAU.GT.2..AND.TAUP.GT.2..AND.I.NE.100) GO TO 29
5430=      PIR=PI*B(I,NU)
5440=      RP1 = R(I) + R(I+1)
5450=      UMAX = TAU * SQRT( RP1 / RM1)
5460=      UMAX2 = UMAX + UMAX
5470=      IF (R(I).LT.RSFEAR(NU)) GO TO 20
5480=      GO TO 25
5490=      20 SINSR=1.
5500=      GUS=G(UMAX)

```

```

5500=      GUS=G(UMAX)
5510=      HUS=H(UMAX)
5520=      GO TO 30
5530= 25 S1NSQ = (RSFEDR(HU)/R(1))**2
5540=      US = (TAU/RM1)*SQRT(R(I+1)**2-RS2)-SQRT(R(I)**2-RS2))
5550=      HUS = H(US)
5560=      GUS = G(US)
5570= 28 F(2,I+1,NU)=PIB+(R(1*I*TAU)**2/(4.*R(I+1)**2)*(((F(2,I
5580=      1,NU)-F(1,I,NU))/SINSQ)*(G(TAU)-GUS))+(F(1,I,NU)-PIB
5590=      2)* (GUS-G(UMAX)))+RM1**2/(2.*R(I+1)*TAU)**2)*((F(1,I
5600=      3+1,NU)-PIB)*(1.-H(UMAX2))-((F(2,I,NU)-F(1,I,NU))/4
5610=      SINSQ)*(H(TAU)-HUS)-(F(1,I,NU)-PIB)*(HUS-H(UMAX)))
5620=      F(2,I+1,NU)=ABS(F(2,I+1,NU))
5630=      GO TO 30
5640= 29 F(2,I+1,NU)=ABS(8.*PI*(B(I,NU)-B(I+1,NU))/(3.*(TAU+TAUP)))
5650= 30 CONTINUE
5660=      X = 0.
5670=      DO 35 NU = 1,MAXNU
5680=      35 X=X+R(2)**2*(F(2,2,NU)-F(1,2,NU))
5690=      DENT(I) = 3.*X / R(2)**3
5700=      DO 50 I = 2,100
5710=      X = 0.
5720=      DO 40 NU = 1,MAXNU
5730=      40 X = X + (R(I)**2 * (F(2,I,NU)-F(1,I,NU))-R(I+1)**2*
5740=      1*(F(2,I+1,NU)-F(1,I+1,NU)))
5750=      50 DENT(I) = (-X*3./(R(I+1)**3 - R(I)**3))
5760=      DO 60 I=1,100
5770=      ER(I) = DENT(I)*DT + ER(I)
5780=      IF(ER(I).LT.6.122E-5) ER(I)=6.122E-5
5790= 60 CONTINUE
5800=      RETURN
5810=      END
5820=C
5830=      FUNCTION G(U)
5840=      REAL MMDEI
5850=      IF(U.GT.225)GO TO 10
5860=      X= EXP(-U) * (1./U**2 - 1./ U)
5870=      Y= MMDEI(2,U,IER)
5880=      G= X + Y
5890=      RETURN
5900= 10 G=0.
5910=      RETURN
5920=      END
5930=C
5940=      SUBROUTINE PLANCK(MAXNU,TEMP,B,WPTEMP,AvgNU)
5950=      DIMENSION TEMP(101),B(101,101),F(9),AVGNU(10)
5960=      REAL K
5970=C----- B=ERG/(SEC*CM**2),H=ERG-SEC,K=ERG/KELVIN,X=Y=HH=AVGNU(I)=HZ
5980=      DATA H,K,C/6.626E-27,1.381E-16,3.E10/
5990=      A(U,L) = H * U / (K * TEMP(L))
6000=      PK(U,R) = 2.*H * U**3 / (C**2 * (EXP(R) - 1))
6010=      X = WPTEMP * 2.418E18 / FLOAT(MAXNU)
6020=      Y = WPTEMP * 2.418E15
6030=      HH = (X-Y)/2.
6040=      AVGNU(1) = (X+Y)/2.
6050=      IF(MAXNU.EQ.1) GO TO 30

```

```

6050= IF(MAXNU.EQ.1) GO TO 30
6060= DO 5 I = 2,MAXNU
6070= 5 ANGNU(I) = ANGNU(I-1) + X
6080= DO 20 NU = 1,MAXNU
6090= Z = Y
610= Y = Y + X
6110= DO 20 I = 1,100
6120= D = A(Z,I)
6130= IF(D.GT.225.) F(1) = 0
6140= IF(D.LE.225.) F(1) = FK(Z,D)
6150= D = A(Y,I)
6160= IF(D.GT.225.) F(9) = 0.
6170= IF(D.LE.225.) F(9) = FK(Y,D)
6180= DO 10 J= 2,8
6190= Z = Z + HH
6200= D = A(Z,I)
6210= IF(D.GT.225.) F(J) = 0,
6220= IF(D.LE.225.) F(J) = FK(Z,D)
6230= 10 CONTINUE
6240= 20 B(I,NU) = HH/3. * (F(1)+F(9)+4.* (F(2)+F(4)+F(6)+F(8))+2. *
6250= 1*(F(3)+F(5)+F(7)))/(X-Y)
6260= GO TO 50
6270= 30 DO 40 I = 1,100
6280= B(I,1)=5.6686E-5*TEMP(I)**4
6290= 40 CONTINUE
6300= 50 CONTINUE
6310= RETURN
6320= END
6330=C
6340= FUNCTION AMU(D,T,ANU,RHO)
6350= REAL MU(5)
6360= DIMENSION TEMP(5)
6370= DATA (TEMP(I),I=1,5),(MU(J),J=1,5)/1.E3,1.E4,1.E5,1.E6,1.E7,1.E-1,
6380= 1,1.91E-10,1.268E-8,1.26E-6,1.27E-6/
6390= IF (T.LE.1.E3) GO TO 10
6400= IF (T.GE.1.E7) GO TO 20
6410= GO TO 30
6420= 10 AMU=7.143E-2*D/RHO
6430= RETURN
6440= 20 AMU=6.25E-9*D/RHO
6450= RETURN
6460= 30 I=1
6470= IF(T.GT.1.E4) I=2
6480= IF(T.GT.1.E5) I=3
6490= IF(T.GT.1.E6) I=4
6500= X=ALOG(1./MU(I))*((ALOG(TEMP(I+1))-ALOG(T))/(ALOG(TEMP(I+1))
6510= 1-ALOG(TEMP(I))))+ALOG(MU(I+1))*(ALOG(T)-ALOG(TEMP(I)))
6520= 2/(ALOG(TEMP(I+1))-ALOG(TEMP(I)))
6530= IF(X.GT.225) X=225.
6540= ANU=EXP(-X)*1/RHO
6550= RETURN
6560= END
6570=C
6580= SUBROUTINE RADSET(MAXNU,DT,WTEMP,TEMP,TSTART,D,E1,YKT
6590= 1,ERY,AMASS,R)
6600= DIMENSION AMASS(101),R(101)

```

```

6600=      DIMENSION AMASS(101),R(101)
6610=      DIMENSION TEMP(101),ET(101),U(101),ER(101)
6620=      TIME,KELV,NU,T,EI,DEUT,ER,TEMP,KEV,0.67CH3
6630=      DO 10 I = 2,100
6640=      ER(1)=6.122E-5
6650=      EI(1) = 3.308E6
6660=      AMASS(1)=D(1)*4./3.*ACOS(-1.)*(R(I+1)**3-R(I)**3)
6670=      10 TEMP(I) = 300.
6680=      TSTART = 1.E-7
6690=      READ*,MAXNU
6700=      PRINT*, " NUMBER OF FREQUENCY GROUPS IS: ",MAXNU
6710=      CALL TEMPO(YKT,R(2),T,EIZERO,ERZERO)
6720=      WPTEMP=8.617E-8*T
6730=      PRINT*, "INITIAL CELL TEMP = ",T,"KELVIN, OR ",WPTEMP," KEV"
6740=      EI(1)=EIZERO
6750=      TEMP(1)=T
6760=      ER(1)=ERZERO
6770=      D(1)=0.3386
6780=      AMASS(1)=1.E6
6790=      RETURN
6800=
6810=C
6820=      SUBROUTINE TEMPO(YKT,R,T,D,C)
6830=      R=89.
6840=      A=YKT*4.18E19
6850=      TLO=1.E3
6860=      THI=1.E8
6870=      10 T=(THI+TLO)/2.
6880=      B=2.E14*T
6890=      C=5.6686E-7*T**4
6900=      D = C + D
6910=      IF(A.GT.B) TLO=T
6920=      IF(A.LT.B) THI=T
6930=      IF(ARS(A-B).GE.0.0001*A) GO TO 10
6940=      C=7.558E-15*T**4
6950=      D=1.103E4*T**16.4
6960=      20 RETURN
6970=      END
6980=C
6990=      SUBROUTINE WRITER(TEMP,P,D,EI,X,DEUT,ER,F)
7000=      DIMENSION TEMP(101),DEUT(101),EI(101),P(101),D(101),X(101)
7010=      DIMENSION ER(101),F(2,101,10)
7020=      PRINT 100
7030=      DO 10 I = 1,20
7040=      J=1
7050=      Z=F(1,I,J)
7060=      S Y=F(2,I,J)
7070=      10 PRINT 200, I,X(I),TEMP(I),P(I),D(I),EI(I),DEUT(I),ER(I),Z,Y
7080=      RETURN
7090=      100 FORMAT (//,2X,"I",10X,"X",10X,"TEMP",10X,"PRESSURE",5X,"DENSITY",
7100=      110X,"EI",10X,"DEUT",10X,"ER",10X,"F(-)",10X,"F()",//)
7110=      200 FORMAT (2X,I2,9(2X,E12.5))
7120=      END
7130=C
7140=      FUNCTION TEMPER(EI,T,U)
7150=      Y=ZSTAR(T) + 1.

```

```

7150=      Y=ZSTAR(T)+1.
7160=      U=1.
7170=      IF(T.GT.2.E3) Q=2.
7180=      TEMPER=1.169E-7*E1*U/(Q*Y)
7190=      RETURN
7200=      END
7210=C
7220=      FUNCTION ZSTAR(T)
7230=      IF(T.LE.2.E4) ZSTAR=0.
7240=      IF(T.GE.1.E6) ZSTAR=2.
7250=      IF(T.GT.2.E4.AND.T.LT.1.E6) GO TO 10
7260=      RETURN
7270=      10 ZSTAR=( ALOG10(T)-4.301)*4.
7280=      RETURN
7290=      END
7300=C
7310=      FUNCTION H(U)
7320=      IF(U.GT.225.) GO TO 10
7330=      H=EXP(-U)*(1.+U)
7340=      RETURN
7350=      10 H=0.
7360=      RETURN
7370=      END
7380=C
7390=      FUNCTION EIA(P,D,RHO)
7400=C----- GUESS GAMMA MINUS ONE -----
7410=      GM1=.28
7420=      DO 30 I=1,10
7430=C----- COMPUTE AN INTERNAL ENERGY -----
7440=      EI=P/(GM1*D)
7450=C----- COMPUTE A NEW GAMMA MINUS ONE -----
7460=      GM1=VGAMMA(EI,D,RHO)-1.
7470=C----- COMPUTE A PRESSURE -----
7480=      P2=GM1*INDEXI
7490=C----- COMPARE PRESSURES -----
7500=      IF(ABS(P-P2).LE..001*P)GO TO 40
7510=C----- GAMMA IS CORRECT WHEN THE PRESSURES AGREE -----
7520=      30 CONTINUE
7530=      PRINT*, "I=",I
7540=      40 EIA=EI
7550=      RETURN
7560=      END

```

VITA

Douglas P. Wade was born on 25 April 1952 in San Antonio, Texas. He graduated from Palo Verde High School in Tucson, Arizona in 1970. He attended the University of Arizona at Tucson graduating May 1974 with a Bachelor of Science degree in Nuclear Engineering. While at the University of Arizona he attended ROTC, and was commissioned upon graduation. Upon completion of missile training in November of 1974, he served as a Minuteman III crew commander and Wing Instructor for the 321st Strategic Missile Wing at Grand Forks AFB, North Dakota. In November of 1977 he was assigned to the Foreign Technology Division (FTD) at Wright-Patterson AFB, Ohio. He performed as an intelligence analyst until entering the School of Engineering, Air Force Institute of Technology in August 1979.

Permanent Address: 5942 E. 24th St.  
Tucson, Arizona 85711

## UNCLASSIFIED

SECURITY CLASSIFICATION OF THIS PAGE (When Data Entered)

REPORT DOCUMENTATION PAGE		READ INSTRUCTIONS BEFORE COMPLETING FORM
1. REPORT NUMBER AFIT-TR-81-10	2. GOVT ACCESSION NO. AD-100637	3. RECIPIENT'S CATALOG NUMBER
4. TITLE (and Subtitle) <b>RADHOT: A RADIATION HYDRODYNAMICS CODE FOR WEAPON EFFECTS CALCULATION</b>		5. TYPE OF REPORT & PERIOD COVERED <b>Master's Thesis</b>
7. AUTHOR(s) <b>Douglas P. Wade Captain USAF</b>		8. CONTRACT OR GRANT NUMBER(s)
9. PERFORMING ORGANIZATION NAME AND ADDRESS <b>Air Force Institute of Technology Wright-Patterson AFB, Ohio 45433</b>		10. PROGRAM ELEMENT, PROJECT, TASK AREA & WORK UNIT NUMBERS
11. CONTROLLING OFFICE NAME AND ADDRESS <b>Air Force Institute of Technology Wright-Patterson AFB, Ohio 45433</b>		12. REPORT DATE <b>Mar 81</b>
14. MONITORING AGENCY NAME & ADDRESS (if different from Controlling Office)		13. NUMBER OF PAGES <b>102</b>
		15. SECURITY CLASS. (of this report) <b>UNCLASSIFIED</b>
		15a. DECLASSIFICATION DOWNGRADING SCHEDULE
16. DISTRIBUTION STATEMENT (of this Report)  <b>Approved for public release; distribution unlimited</b>		
17. DISTRIBUTION STATEMENT (of the abstract entered in Block 20, if different from Report)  <i>Fredric C. Lynch</i> <b>22 JUN 1981 FREDRIC C. LYNCH, Major, USAF</b> D: Public Release		
18. SUPPLEMENTARY NOTES  <b>Air Force Institute of Technology (ATC) Wright-Patterson AFB, OH 45433</b>		
19. KEY WORDS (Continue on reverse side if necessary and identify by block number)		
20. ABSTRACT (Continue on reverse side if necessary and identify by block number)  <b>RADHOT is a one-dimensional Lagrangian radiation-hydrodynamics computer code developed from a scheme described by John Zinn of LASL. The transport scheme described by John Zinn and incorporated into RADHOT requires just two passes thru the mesh to determine fluxes and energy deposition rates. The scheme assumes local thermodynamic equilibrium for each cell, and also assumes that the thermal radiation flux contribution in a given direction at any point has one of two values depending upon whether a ray in that</b>		

UNCLASSIFIED

SECURITY CLASSIFICATION OF THIS PAGE (If Other Data Entered)

direction intersects the source region.

The RADHOT code currently suffers from a lack of valid opacity data. The code as currently written is extremely slow and expensive to run. A user's guide and a listing the code are provided as a starting point for future work.

UNCLASSIFIED

SECURITY CLASSIFICATION OF THIS PAGE (If Other Data Entered)

